(5.23)

Numerical Modeling. Empirical relationships such as those given by Anderson and Zubov contain implicit assumptions regarding $F_w(t)$ and $h_s(t)$. As we have seen above, variations in these quantities can have a large effect on the response of H to changes in θ. Application of such relationships to areas with different ocean heat flux or snowfall patterns (e.g., the Central Arctic and Southern Ocean) is thus questionable. Suitable forecasting equations for these areas should be developed independently, either directly from ice growth measurements or indirectly from heat balance data and theoretical models. It is the latter approach we shall discuss below.

Let us consider a slab of young ice of thickness H, overlain by a layer of snow of thickness h_s. We shall assume that the surface is in thermal equilibrium, i.e., heat gain is exactly balanced by heat loss. We can then write a heat balance for the upper boundary

$$(1 - \alpha)F_r - I_o + F_L - F\uparrow + F_s + F_e + F_c + F_m = 0 \qquad (5.24)$$

where F_m is the heat loss due to melting of ice or snow, and

$$F_m = \left[\rho L \frac{d(H + h_s)}{dt}\right]_o . \qquad (5.25)$$

When the surface temperature is below freezing, $F_m = 0$. If T_o is at the melting point, any surplus of energy flux toward the surface will be balanced by melting and a change in $H + h_s$. Since we are considering the case of young ice, we will assume that temperature gradients in the ice and snow are linear, so that

$$F_c = \frac{k_i k_s}{k_i h_s + k_s H}(T_f - T_o) = \gamma(T_f - T_o) \qquad (5.26)$$

where γ is the thermal conductance of the combined ice/snow slab. Substituting eqs. (5.1), (5.10), (5.12), (5.14), (5.25) and (5.26) into eq. (5.24), the upper boundary condition can be written

$$(1 - \alpha)(1 - i_o)F_r + F_L - \varepsilon_L \sigma T_o^4 + K_s(T_a - T_o)$$
$$+ K_e(re_{sa} - e_{so}) + \gamma(T_f - T_o) + \left[\rho L \frac{d(H + h_s)}{dt}\right]_o = 0 \qquad (5.27)$$

where $K_s = \rho_a C_p C_s u$ and $K_e = .622\,\rho_a L C_e u/P$. Because the albedo of cold, thin ice increases rapidly with thickness, problems involving spring ice formation may need to take this change into account. An approximate relationship between α and H can be derived from the

observations of Weller (1972).

$$\alpha(H) = .44\ H^{.28} + .08$$

where H is in meters and $0<H<.8$ m.

The lower boundary condition is obtained from eqs. (5.20) and (5.26)

$$-\rho_i L \left(\frac{dH}{dt}\right)_H = \frac{k_i k_s}{k_i h_s + k_s H} (T_f - T_o) + F_w \quad . \tag{5.28}$$

Equations (5.27) and (5.28) form the young ice model. The rate of growth for any given values of H, h_s, and F_w can be calculated from eq. (5.28) if T_o is known. T_o can be obtained from eq. (5.27) by specifying F_r, F_L, T_a, h_s, u, and r. Growth of an ice cover from arbitrary initial conditions can be calculated in this way for any time dependent, thermal forcing.

The advantage of this approach over empirical formulas is generality. Providing that sufficient information is available regarding the thermal forcing, eqs. (5.27) and (5.28) can be used not only to describe heat exchange in areas such as the Central Arctic, Southern Ocean, and SSIZ, but also to calculate ice decay or growth when the radiation balance is not close to zero. It can be argued that there are too many unknown variables for this approach to be useful in a routine forecasting mode. Data on F_L, for example, will almost never be available. In practice, however, we can reduce the number of variables significantly. By using the parameterizations for F_r and F_L discussed in Section 5.2 (eqs. 5.2, 5.5 and 5.6), incident radiation at a particular location can be expressed in terms of cloudiness and air temperature. During most of the year F_e is small relative to F_s and r can be taken as 0.9 or 0.95 with little error. Wind speed tends to be relatively constant over much of the Arctic Basin and an average value of 5 m sec^{-1} is frequently used in calculating the turbulent fluxes. The remaining quantities which must be specified are T_a, C, h_s, and F_w. The first three can be measured directly, estimated from climatology, or, in the case of cloudiness, determined from satellite data. F_w cannot be measured directly and must instead be inferred from salinity and temperature changes in the upper ocean or from its effect on ice thickness.

We have described here a practical method of estimating young ice growth which includes an explicit dependence on those factors which are most likely to undergo large changes from one region to another. Known differences in climatic or oceanographic conditions can therefore be taken directly into account. The model can be used to generate simple predictive equations like those of

Zubov and Anderson a
tudes of the input pa
ice. Probably the g
is that it provides a
is available.

5.3.3 Multiyear and

A fundamental st
was the assumption
which caused ice thic
in thermal forcing a
ice, this assumption
through multiyear a
surface temperature d
in ice growth. The
thermal history than
instant of time. In
be observed at the
place at the surfac
growing vigorously i
thickness due to b
temperature field obs
It is evident from
September is not felt
Changes in surface t
ly damped out by the

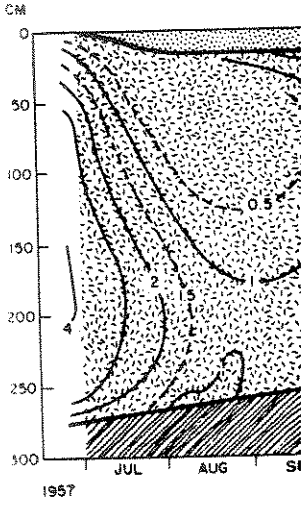

Fig. 17. Temperatu
al ice in

Zubov and Anderson and to learn how uncertainties in the magnitudes of the input parameters affect the predicted growth of the ice. Probably the greatest strength of the theoretical approach is that it provides a framework for utilizing whatever information is available.

5.3.3 Multiyear and Thick First Year Ice

A fundamental step in the development of the young ice model was the assumption of a linear temperature gradient in the ice which caused ice thickness to respond immediately to any changes in thermal forcing at the surface. Although reasonable in thin ice, this assumption is inadequate to describe heat transport through multiyear and thick first year ice where changes in surface temperature do not necessarily result in immediate changes in ice growth. The growth of thicker ice depends more on its thermal history than on the surface heat balance at any particular instant of time. In the early summer, for example, accretion can be observed at the underside of the ice while melting is taking place at the surface. Similarly, in October when young ice is growing vigorously in leads, thick ice is generally decreasing in thickness due to bottom melting. Figure 17 shows the annual temperature field observed in perennial ice in the Central Arctic. It is evident from this that the fall cooling which begins in September is not felt at the bottom of the ice until mid-December. Changes in surface temperature like the January warming are largely damped out by the time they reach the bottom. Even during the

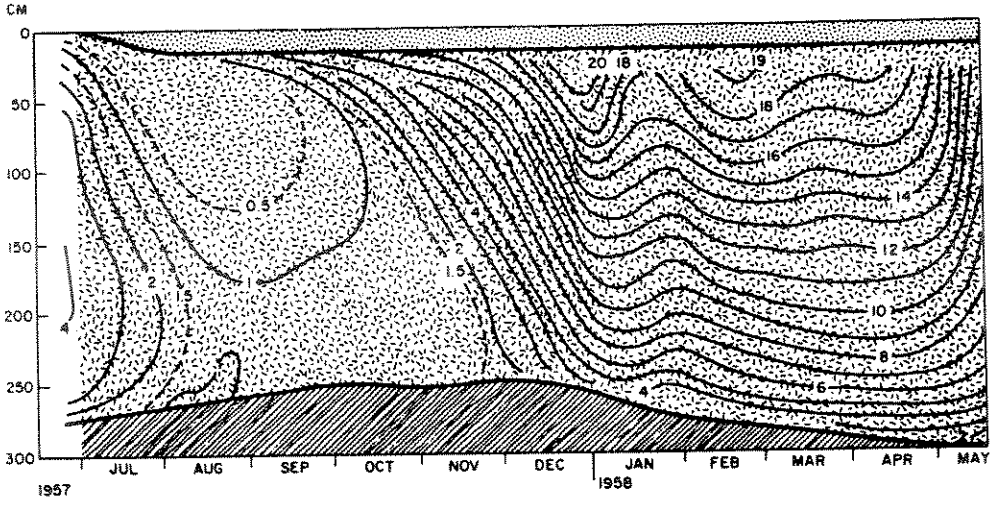

Fig. 17. Temperature and thickness variations observed in perennial ice in the Central Arctic. (After Untersteiner, 1961.)

middle of the winter there appear to be significant departures from linearity within the ice.

Figure 18 shows theoretical predictions of how growth rates (f) in thicker arctic ice vary with season and thickness. The curves demonstrate that differences in thermal mass strongly affect how the ice responds to changes at the upper surface. In November, over 2 months after freeze-up, ice thicker than about 3 m continues to ablate because the fall cooling has not yet begun to affect the lowest part of the ice. Above 4 m there is a slight decrease in ablation rate with increasing thickness, suggesting that the effects of summer warming have not yet reached a maximum. By January it is evident that the fall cooling has penetrated all but the thickest ice. During April there is typically a 5°C increase in T_a which is reflected in decreased growth rates in ice thinner than 3 m. Growth rates in thicker ice, however, are unaffected by this warming and increase in response to continued cooling near the bottom. A 10-15°C increase in T_a during May causes a sharp drop in f for the thinner ice, while f(H>5 m) again increases. The magnitude of the spring warming effect decreases with increasing thickness and explains the predicted increase in f between 1-3 m. Clearly the assumption of a linear temperature profile is invalid for thicker ice.

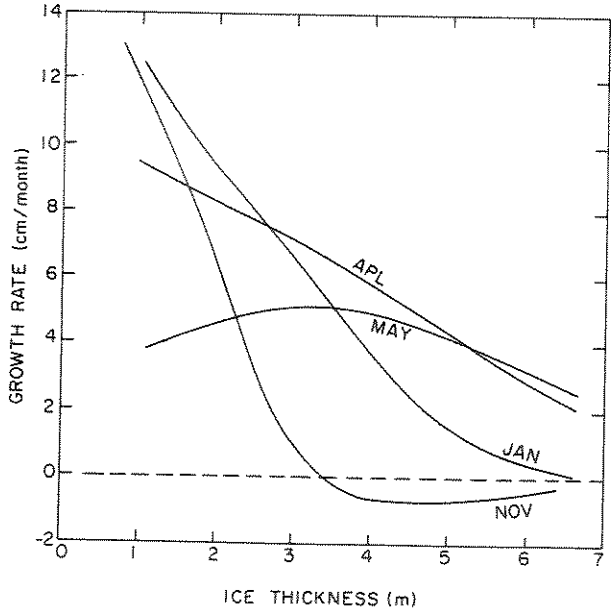

Fig. 18. Growth rates in multiyear arctic sea ice as a function of thickness and season according to the theoretical model of Maykut and Untersteiner (1971).

THE SURFACE HEAT AND MA

Brine pockets are
linearities in the tem
the ice causes some of
and slowing the overal
cause melting of ice s
in the rate of warming,
which retard temperatu
these temperature depe
heat of sea ice (c_i)
alter the temperature
heat associated with
Ono (1967) derived a
temperatures above -8

$$c_i = c_o + aT_i + \frac{b}{}$$

where T_i is in °C, a
c_o = 2113 J kg^{-1} $°C^{-1}$
form which gives sim
Untersteiner (1961):
kg^{-1}. Tables and an
colder ice (Anderson,
largest changes in c_i
the magnitude of these
ditions, c_i varies by
the melting point. Bc
of the vertical variat

The dramatic inc
means that mass change
increasing share of t
difficult to change T.
equations for c_i and
is not the case, how
$S_i \to 0$. Whereas pure
which phase transitio
produces internal phas
a given salinity the
cannot exist without
(1967), $T_m \simeq -0.05411$
the temperature of sea

General Thermodyn
on the treatment of t
detailed sea ice model
and internal heating
and temperatures with
heat conduction equati

significant departures

is of how growth rates
and thickness. The
thermal mass strongly
he upper surface. In
ce thicker than about
ling has not yet begun
4 m there is a slight
thickness, suggesting
yet reached a maximum.
ing has penetrated all
s typically a 5°C in-
l growth rates in ice
er ice, however, are
response to continued
ase in T_a during May
while f(H>5 m) again
ming effect decreases
edicted increase in f
a linear temperature

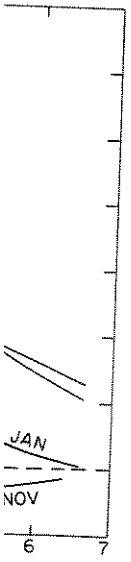

a ice as a function
to the theoretical
1).

Brine pockets are an important factor contributing to nonlinearities in the temperature profile of thick ice. Cooling of the ice causes some of the brine to freeze, releasing latent heat and slowing the overall rate of cooling; increasing temperatures cause melting of ice surrounding the brine pockets and a decrease in the rate of warming. Brine pockets thus act as thermal buffers which retard temperature changes in either direction. Because of these temperature dependent changes in brine volume, the specific heat of sea ice (c_i) must include not only the heat required to alter the temperature of the ice and brine, but also the latent heat associated with melting and freezing in the brine pockets. Ono (1967) derived a theoretical expression for c_i applicable to temperatures above -8 °C,

$$c_i = c_o + aT_i + \frac{b\,S_i}{T_i^2}$$

where T_i is in °C, a = 7.53 J kg^{-1} °C^{-2}, b = 0.018 MJ °C kg^{-1}, and c_o = 2113 J kg^{-1} °C^{-1} is the specific heat of pure ice. A simpler form which gives similar results is the empirical formula of Untersteiner (1961): $c_i = c_o + \zeta S_i/T_i^2$, where ζ = 0.0172 MJ °C kg^{-1}. Tables and analytical expressions are also available for colder ice (Anderson, 1958; Schwedtfeger, 1963). As with k_i, the largest changes in c_i occur at temperatures above -4 to -6°C, but the magnitude of these changes are much larger. Under natural conditions, c_i varies by a factor of 10-20 as the ice warms toward the melting point. Both k_i and c_i are dependent on depth because of the vertical variations in ice salinity.

The dramatic increase in $c_i(T_i,S_i)$ at temperatures near 0°C means that mass changes within the brine pockets are consuming an increasing share of the available energy, making it increasingly difficult to change T_i. At first glance it would appear that the equations for c_i and k_i predict infinite values as $T_i \to 0$°C. This is not the case, however, because T_i cannot approach 0°C unless $S_i \to 0$. Whereas pure ice has a well-defined temperature (0°C) at which phase transitions occur, sea ice does not. Any change in T_i produces internal phase changes. It can be shown that for ice of a given salinity there is a temperature (T_m) above which the ice cannot exist without completely melting away. According to Ono (1967), $T_m \simeq -0.05411\ S_i$. This is consistent with the claim that the temperature of sea ice can reach 0 °C only if $S_i = 0$.

General Thermodynamic Model. To avoid the limitations imposed on the treatment of thin ice, Maykut and Untersteiner developed a detailed sea ice model which takes into account effects of salinity and internal heating on ice growth. To describe heat transport and temperatures within the ice, they used a modified form of the heat conduction equation

$$\rho_i c_i \frac{\partial T_i}{\partial t} = \frac{\partial}{\partial z}\left(k_i \frac{\partial T_i}{\partial z}\right) + I_o \kappa_i e^{-\kappa_i z} \qquad (5.29)$$

where the last term describes the depth dependent internal heating which occurs in the ice as a result of absorption of penetrating shortwave radiation (see Section 5.2.1). A similar equation was used to describe temperatures in the snow

$$\rho_s c_s \frac{\partial T_s}{\partial t} = k_s \frac{\partial^2 T_s}{\partial z 2} \qquad (5.30)$$

where k_s was assumed to be constant with depth and the I_o term was taken to be negligible because light attenuation in the snow is large and most of the solar energy is absorbed in the upper 0.1 m. This means that I_o in the ice is zero when $h_s > 0$.

Heat conduction at the ice-snow interface was assumed to be equal in both media

$$k_i \left(\frac{\partial T_i}{\partial z}\right)_{h_s} = k_s \left(\frac{\partial T_s}{\partial z}\right)_{h_s} .$$

Equations (5.24) and (5.20) were used for the boundary conditions at the top and bottom of the ice. An important difference between this model and the young ice model described previously is that the conductive heat fluxes at the boundaries depend on the local temperature gradients, hence are generally different at the top and bottom of the slab. A schematic illustration of this model is shown in Figure 19. When the model was driven with estimates of incident energy fluxes and snowfall in the Central Arctic, it provided temperatures and mass changes in good agreement with observations (Figure 20).

A serious drawback to this approach is that the solution to eqs. (5.29) and (5.30) must be obtained by finite difference techniques which involve considerable computer time if good temperature resolution is desired. This makes it impractical to use the full model in many applications which require simultaneous predictions at numerous locations or thicknesses. In an effort to develop a simpler version suitable for numerical climate experiments, Semtner (1976) devised a streamlined numerical method for solving the above equations which required an order of magnitude fewer grid points. He showed that this method produced equilibrium thicknesses which agreed with results from the more elaborate procedures of Maykut and Untersteiner to within about 25 cm over a wide range of environmental conditions. As part of a study of transient

Balance of fluxes

$$(1-\alpha)F_r - I_o + F_L - \varepsilon_L \sigma T_o^4 + F_s + F_e + k_o\left(\frac{\partial T}{\partial z}\right)_o + \left|\rho L \frac{d}{dt}(h+H)\right|_o = 0$$

Heat conduction

$$(\rho c)_s \frac{\partial T_s}{\partial t} = k_s \frac{\partial^2 T_s}{\partial z^2}$$

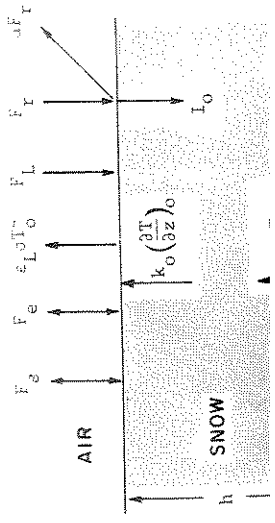

(5.29)

lent internal heating
ɔption of penetrating
similar equation was

(5.30)

and the I_o term was
tion in the snow is
i in the upper 0.1 m.
).

e was assumed to be

: boundary conditions
ɛt difference between
l previously is that
depend on the local
lifferent at the top
ion of this model is
en with estimates of
tral Arctic, it pro-
ɔeement with observa-

that the solution to
ite difference tech-
ime if good tempera-
practical to use the
simultaneous predic-
ı an effort to devel-
climate experiments,
. method for solving
magnitude fewer grid
ıuilibrium thickness-
ıborate procedures of
ɔver a wide range of
study of transient

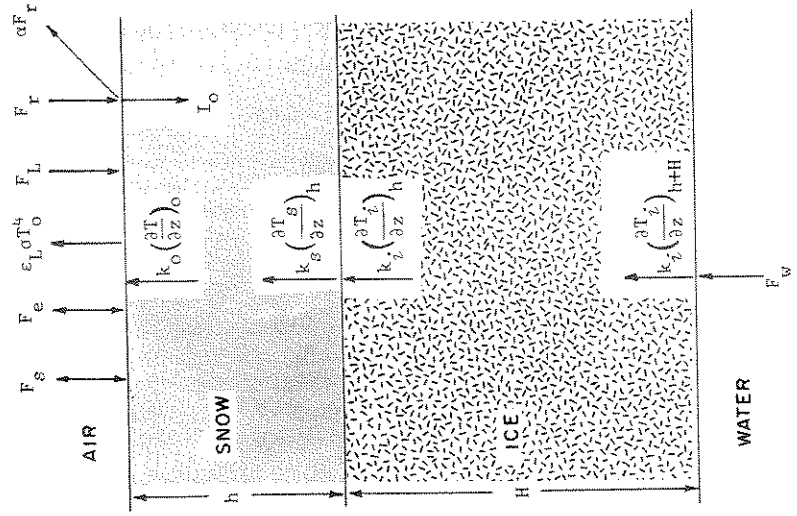

Fig. 19. Schematic illustration of the sea ice model developed by Maykut and Untersteiner (1971).

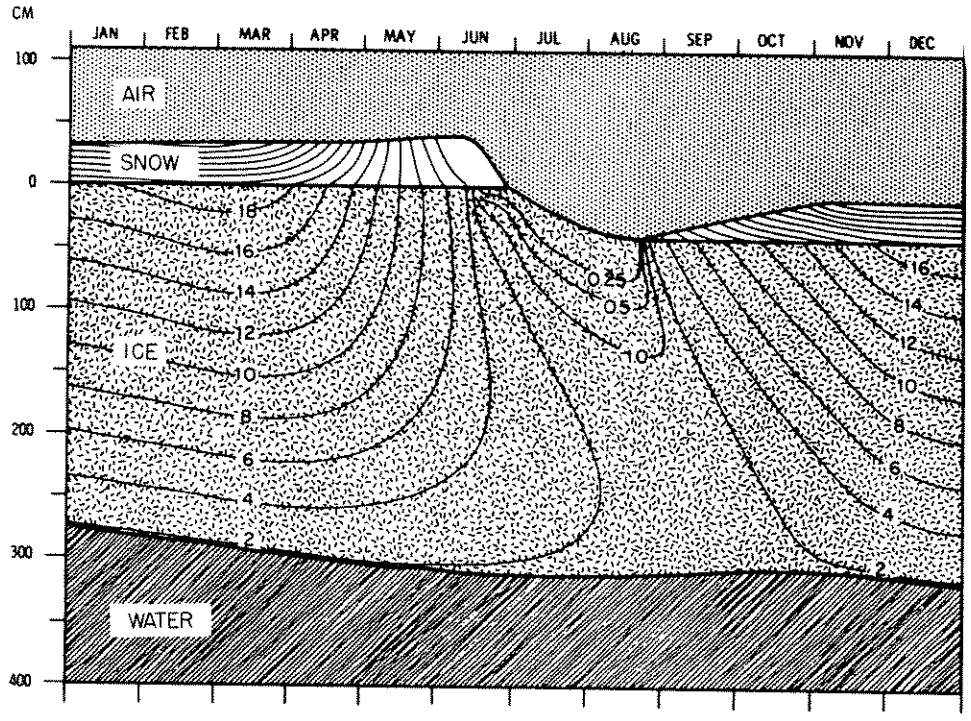

Fig. 20. Predicted values of equilibrium temperature and thickness in the Central Arctic (after Maykut and Untersteiner, 1971).

growth rates in thicker ice, we examined how temperature resolution in the ice affected winter predictions. We found that a linear temperature profile tended to overestimate growth rates during periods of cooling and underestimate them during periods of warming, the effect becoming more pronounced as H increased. About 75% of the error could be removed by including a single internal temperature point, and about 95% by including three interior points. Conditions in the summer and fall were not so simple, with rates depending more on the treatment of the internal heating than on the temperature resolution. While other simplifications involving the thermal properties or the boundary conditions can also be made, there is no single form of the model which will be equally useful in all situations. Different applications require the development of different versions, depending on the variables of interest, the desired temporal and spatial resolution, and the data available.

THE SURFACE HEAT AND MASS

5.3.4 Response of Sea Ic

Because of its prob
great deal of interest
changes in thermal forcin
thickness might be artif
described in the precedi
quantitatively evaluate t
factors and the efficien
The effects of a partic
the model through many an
ture and thickness patt
when the net annual growt
annual ice ablation at t
surface ablation, for ex
the larger bottom accre
gradient exactly balances
a decrease in surface abl
The time required for th
final equilibrium thickn
is small (1 m) and tens o

The turbulent transf
been subject to numerous
tions in F_w are an inte
numerous schemes for art
ice in the Arctic depend
proposals is difficult to
of the sensitivity of
(1971) carried out a seri
to vary between 0 and 8
conditions, perennial ic
5-1/2 to 6 meters. The
exceeds about 7 W m^{-2}.
obtained assuming that
another series of unpubl
variations have little
all the oceanic heat flu
and fall, H_e was somew
constant F_w case, but sh
following summer becau
essentially unchanged.
mates, F_w = 2 W m^{-2} pr
variations in H_e and fie
we shall discuss in mor
areas of perennial ice i
tration than to the amo
from the Atlantic Ocean
modification methods and
tions in this heat exchan

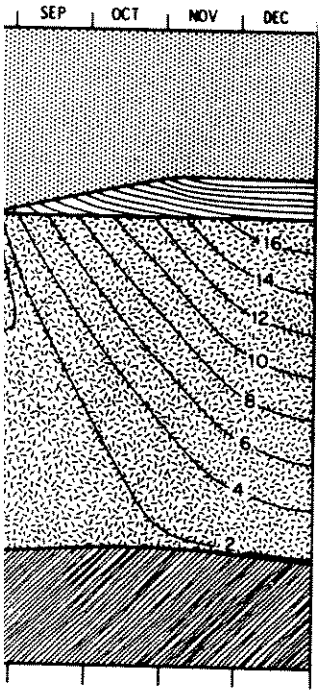

emperature and thick-
(after Maykut and

w temperature resolu-
. We found that a
stimate growth rates
iem during periods of
s H increased. About
ng a single internal
iding three interior
were not so simple,
the internal heating
other simplifications
ndary conditions can
model which will be
applications require
ing on the variables
resolution, and the

5.3.4 Response of Sea Ice to Changes in Thermal Forcing

Because of its probable role in climate, there has been a great deal of interest in the long term response of the ice to changes in thermal forcing and in techniques whereby ice extent or thickness might be artificially modified. The complete ice model described in the preceding section provides a convenient way to quantitatively evaluate the relative importance of various climatic factors and the efficiency of different modification techniques. The effects of a particular change can be studied by integrating the model through many annual cycles until an equilibrium temperature and thickness pattern is obtained. Equilibrium is reached when the net annual growth at the bottom of the ice equals the net annual ice ablation at the surface. An increase in the amount of surface ablation, for example, would force the ice to thin until the larger bottom accretion produced by the steeper temperature gradient exactly balances the increased mass loss at the surface; a decrease in surface ablation would provoke the opposite response. The time required for the ice to reach equilibrium depends on the final equilibrium thickness (H_e), being only a few years when H_e is small (1 m) and tens of years when H_e is large (> 6 m).

The turbulent transfer of heat from the ocean to the ice has been subject to numerous estimates and speculations. Wide variations in F_w are an integral part of some ice age theories, and numerous schemes for artificially influencing the extent of the ice in the Arctic depend on changing F_w. The feasibility of such proposals is difficult to establish without quantitative knowledge of the sensitivity of the ice to F_w. Maykut and Untersteiner (1971) carried out a series of simulations in which F_w was allowed to vary between 0 and 8 W m^{-2} (Figure 21). Under present surface conditions, perennial ice can only grow to a maximum thickness of 5-1/2 to 6 meters. The ice cover melts completely away when F_w exceeds about 7 W m^{-2}. The results shown in Figure 21 were obtained assuming that F_w was constant throughout the year, but another series of unpublished calculations indicate that temporal variations have little net effect on the ice. For example, when all the oceanic heat flux was added to the ice during the summer and fall, H_e was somewhat thinner during the fall than in the constant F_w case, but showed an overall thickness increase by the following summer because of enhanced winter growth; H_e was essentially unchanged. In agreement with other independent estimates, F_w = 2 W m^{-2} provides the best agreement between seasonal variations in H_e and field observations in the Central Arctic. As we shall discuss in more detail later, it now appears that F_w in areas of perennial ice is more closely related to the ice concentration than to the amount of heat carried into the Arctic Basin from the Atlantic Ocean. If this is the case, then artificial modification methods and ice age theories which depend on variations in this heat exchange should be reexamined.

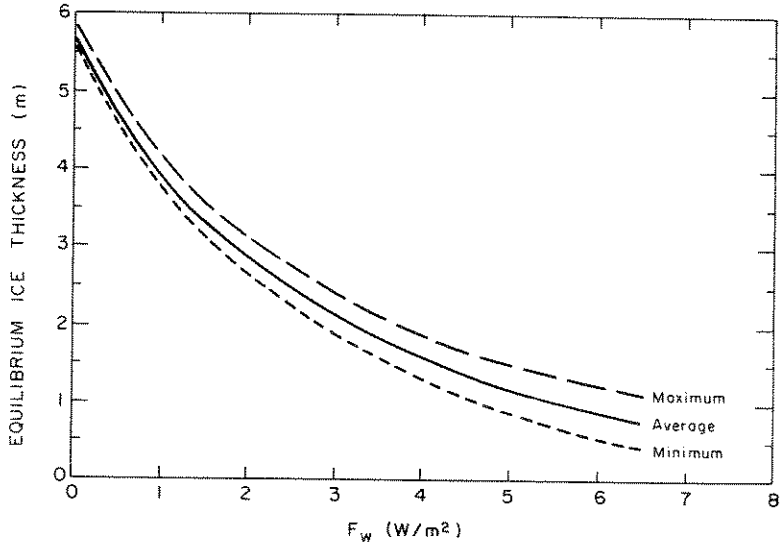

Fig. 21. Equilibrium thickness of arctic sea ice as a function of of oceanic heat flux. Average annual thickness, as well as the absolute annual maximum and minimum, are shown (after Maykut and Untersteiner, 1971).

Because of the magnitude of the incoming shortwave radiation, a small reduction in the surface albedo would provide a large increase in available energy at the surface. It has been frequently suggested that the ice pack might be removed by lowering its albedo through the dispersal of some dark substance like coal dust on its surface. Although some small scale albedo modification experiments have been performed on sea ice (Arnold, 1961), it is not known how feasible such efforts would prove to be on a large scale. Numerical experiments indicate that a 10% reduction in albedo (from 0.64 to 0.54) during the melt season would reduce H_e to about 1 m, while a 20% decrease would result in the complete melting of the ice cover after about three years. Thus, as expected, we see that relatively small changes in α have a large effect on H_e. However, due to the presence of melt ponds, area-averaged summer albedos on perennial ice probably already lie in the .50-.55 range and we must ask why H_e appears to be closer to 3 m than to 1 m over much of the Arctic Basin. The answer is that melt ponds seem to have little net effect on the mass balance of perennial ice. Most of the increase in absorbed shortwave radiation goes into deepening of the ponds and increasing the brine volume in the underlying ice. Fall and winter cooling cause the ponds to refreeze, increasing the ice mass and releasing their stored heat to the atmosphere. This cycle of melting and

refreezing in the ponde
surrounding ice, hence

Modifying the sur
penetrating shortwave
therefore carried out
I_o (Figure 22). The r
internal heating increa
the energy available fo
analogy with the melt
in the ice as latent h
over an annual cycle.

Winter temperature
creased by as much as
direction of future c
concern regarding the
atmosphere. Theoretica
suggest that the expec
the next century could
the Arctic. Relatively
Parkinson and Kellogg,
4–5°C warmer than pre
Ocean, at least during
be extremely sensitive
true, one must be cau
quoted above. The rapi
is possible to maintai
next to the melting ice
and latent heat to th
clearly unrealistic.
of atmospheric warming

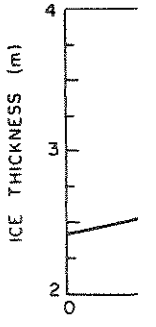

Fig. 22. Average equi
function of i

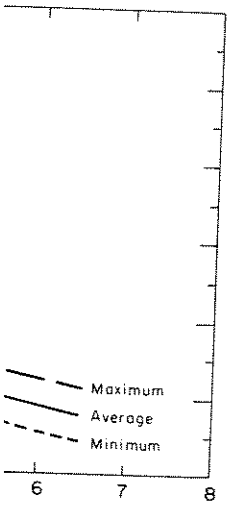

ice as a function of
al thickness, as well
d minimum, are shown
).

shortwave radiation,
provide a large in-
t has been frequently
ved by lowering its
stance like coal dust
albedo modification
Arnold, 1961), it is
ve to be on a large
10% reduction in al-
n would reduce H_e to
in the complete melt-
Thus, as expected,
ve a large effect on
ponds, area-averaged
already lie in the
to be closer to 3 m
The answer is that
the mass balance of
bed shortwave radia-
ncreasing the brine
r cooling cause the
nd releasing their
le of melting and

refreezing in the ponded areas does not have a large effect on the surrounding ice, hence H_e remains about the same.

Modifying the surface of the ice also alters the amount of penetrating shortwave radiation. A series of calculations were therefore carried out to determine the sensitivity of the ice to i_o (Figure 22). The results showed that increasing the amount of internal heating increased H_e, primarily because of a decrease in the energy available for melting at the upper surface. In direct analogy with the melt ponds, shortwave energy absorbed and stored in the ice as latent heat had little impact on the mass balance over an annual cycle.

Winter temperatures in the polar regions appear to have increased by as much as 10-15°C from the ice age minimums. The direction of future changes is of course unknown, but there is concern regarding the possible effects of increasing CO_2 in the atmosphere. Theoretical studies (e.g., Manabe and Wetherald, 1980) suggest that the expected doubling in CO_2 concentrations during the next century could lead to temperature increases of 7-8°C in the Arctic. Relatively simple heat balance models (Budyko, 1974; Parkinson and Kellogg, 1979) predict that summer temperatures only 4-5°C warmer than present would result in an ice-free Arctic Ocean, at least during the summer. The ice cover thus appears to be extremely sensitive to T_a. While this statement is certainly true, one must be cautious about using predictions such as those quoted above. The rapid ice decay relies on the assumption that it is possible to maintain temperature gradients of several degrees next to the melting ice, thereby pumping large amounts of sensible and latent heat to the surface for months at a time. This is clearly unrealistic. What is needed to evaluate the consequences of atmospheric warming during the summer is a coupled atmospheric

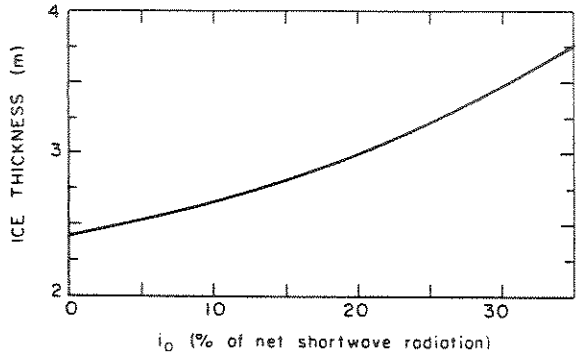

Fig. 22. Average equilibrium thickness of arctic sea ice as a function of i_o (after Maykut and Untersteiner, 1971).

model that will more realistically describe the downward transport of heat from the atmosphere to the ice.

Accompanying changes in temperature are likely to be changes in cloudiness, incident radiation, and precipitation. While we don't know exactly how large such changes might be, it is possible to get some idea of what could happen by simple parameter studies. Figure 23, for example, shows theoretical predictions of the relationship between X_e and h_s. Snow accumulations from 0 to twice the present value of 40 cm have a minimal effect on H_e. This is surprising because variations in h_s alter surface ablation and ice temperatures, suggesting the potential for substantial changes in H_e. The reason this doesn't happen is that the two major effects oppose one another. With less snow, colder ice temperatures promote bottom accretion, but at the same time the summer snow cover melts away sooner, decreasing the average albedo and extending the duration of ice melting; the result is an increase in both bottom accretion and surface ablation which tends to balance out over the range $0 < h_s < 80$ cm. Above 80 cm, decreasing summer ice ablation becomes the dominant factor and H_e increases rapidly with h_s.

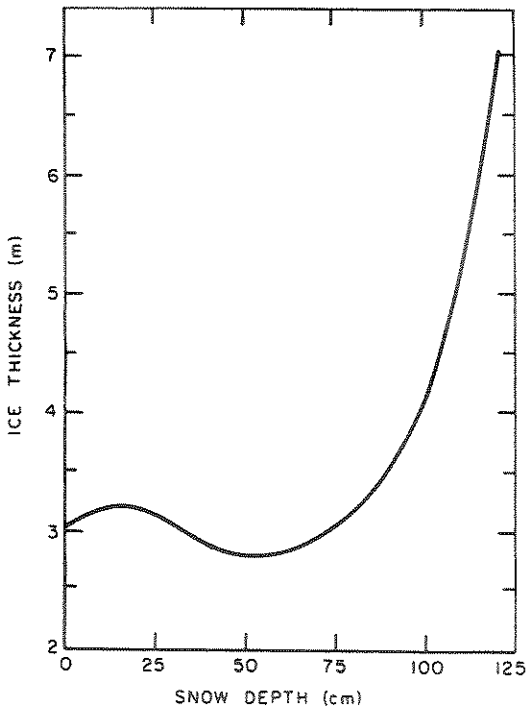

Fig. 23. Average equilibrium thickness of arctic sea ice as a function of maximum annual snow depth; the present day value is 40 cm. (After Maykut and Untersteiner, 1971).

THE SURFACE HEAT AND MA

For any climatic region
fall (about 1.2 m in th
removed during the melt
will be a net annual a
"floating glacier," gr
The combination of a sma
almost any thickness a
the very thick ice found
of Ellesmere Island (Wal

Although we have r
of how variations in c
radiation affect the ic
from the Central Arcti
at what could happen i
cloudiness during the
This is roughly equivale
10% increase in the inc
the net longwave balar
warmer T_o. The increas
the ice forcing H_e to
growth rates to match t
temperatures produced a
case we looked at the
sponding to a decrease
face ablation increase
variations in summer cl
H_e. As with summer a
whether changes in $\bar{C}$ of
a melting ice cover.
situations where variat
radiation fluxes, char
accompanied by changes
heat exchange near the
not describe the total
The most important thi
well we can individual
will not be able to fu
and climate until the
occurring within the s
scale simulations.

5.4 LARGE SCALE HEAT A

In Section 5.2 we
over perennial ice.
almost continual motion
to fracture and expos

be the downward transport

are likely to be changes
recipitation. While we
might be, it is possible
imple parameter studies.
predictions of the rela-
lations from 0 to twice
l effect on H_e. This is
surface ablation and ice
r substantial changes in
at the two major effects
er ice temperatures pro-
me the summer snow cover
albedo and extending the
increase in both bottom
s to balance out over the
sing summer ice ablation
reases rapidly with h_s.

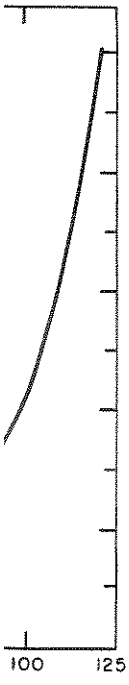

f arctic sea ice as a
depth; the present day
d Untersteiner, 1971).

For any climatic region there will be some critical value of snowfall (about 1.2 m in the central Arctic) which is just able to be removed during the melt season. If h_s exceeds this value, there will be a net annual accumulation of snow and the ice becomes a "floating glacier," growing from above and ablating from below. The combination of a small F_w and high snowfall can produce ice of almost any thickness and has been used to explain the origin of the very thick ice found in Nansen Sound and along the north coast of Ellesmere Island (Walker and Wadhams, 1979).

Although we have not carried out a systematic investigation of how variations in cloudiness, winter temperatures, or incident radiation affect the ice cover, a few miscellaneous calculations from the Central Arctic can be mentioned. In one case we looked at what could happen if there were an increase in the average cloudiness during the winter (October-April) from 0.55 to 0.85. This is roughly equivalent to increasing T_a by 5-6°C. There was a 10% increase in the incoming longwave radiation, but no change in the net longwave balance since $F\uparrow$ increased in response to a warmer T_o. The increase in T_o decreased temperature gradients in the ice forcing H_e to decrease in order to maintain large enough growth rates to match the surface ablation. The increased winter temperatures produced almost a 1 m decrease in H_e. In another case we looked at the ice response to a 10% increase in F_r, corresponding to a decrease in the summer value of $\bar{C}$ of about 0.1. Surface ablation increased by 50%, decreasing H_e by 1.2 m. Small variations in summer cloudiness can thus produce large changes in H_e. As with summer air temperatures, however, it is not clear whether changes in $\bar{C}$ of even 0.1 are reasonable in the presence of a melting ice cover. While these cases attempted to look at situations where variations in C affect only one of the incident radiation fluxes, changes in cloudiness are also likely to be accompanied by changes in snowfall, air temperature and turbulent heat exchange near the surface. The above results therefore do not describe the total response of the system to changes in C. The most important thing to keep in mind is that no matter how well we can individually model the ice, ocean or atmosphere, we will not be able to fully understand the relationship between ice and climate until the various interactions and feedback processes occurring within the system have been included in coupled, large scale simulations.

5.4 LARGE SCALE HEAT AND MASS BALANCE

In Section 5.2 we described the local heat balance observed over perennial ice. We know, however, that the ice pack is in almost continual motion and that strains within the ice cause it to fracture and expose the ocean. Temperature gradients over

winter leads can reach 30 to 40°C over a vertical distance of only a few meters, causing large losses of sensible and latent heat from the ocean. The source of energy for these fluxes is latent heat generated by freezing of the water. As a result, ice production in winter leads is correspondingly large. Continual opening and closing of the ice, combined with continual ice formation and new growth, give rise to a horizontally nonuniform ice cover composed of ice of many different thicknesses. Although subject to similar thermal forcing, the heat and mass balance of each of these different thicknesses is distinct. For example, winter rates of ice growth, turbulent heat exchange with the atmosphere, and salt rejection to the ocean can be up to two orders of magnitude larger over a refreezing lead than over perennial ice. Although decreasing rapidly with increasing ice thickness, these rates can still be an order of magnitude larger over 50 cm ice than over 3 m ice. During the summer there is little thermal distinction between ice of different thicknesses, but leads admit large quantities of shortwave radiation to the upper ocean which ultimately affect the mass balance of the ice pack. Because current estimates of heat exchange and ice production in the Arctic are based largely on measurements made over perennial ice, they do not directly take into account contributions made by thin ice and open water. For some components such as the incident radiation this omission is of little consequence, but for quantities which are sensitive to ice thickness the result may be a serious distortion of the large scale picture. For example, if the ice pack were composed of 99% perennial ice and 1% refreezing leads, winter ice production in the small area covered by leads would be roughly equal to that in the area covered by perennial ice; total ice production for the region would be twice as large as that predicted on the basis of local measurements made only in the thicker ice.

5.4.1 Regional Averaging

Clearly there is a strong coupling between dynamic and thermodynamic processes in the ice. Large changes in the amount of thin ice and open water can occur on time scales of hours to days, producing corresponding changes in the regional heat and mass balance independent of any changes in the incident energy fluxes. Because they do not take into account contributions made by areas of thin ice and open water, data gathered over thick ice do not necessarily provide good estimates of the area-averaged heat and mass fluxes. In most cases such large scale fluxes cannot be measured directly. Instead it is necessary to determine, first, how each component of the heat and mass balance varies with ice thickness and, second, the area covered by ice of any given thickness. The contribution made by a particular thickness category is then found by multiplying the fractional area covered by that category times the magnitude of the flux over that thickness. Summing over all categories yields the large scale total.

To quantify thickness
Thorndike et al. (1975) intr
$g(H)$, called the ice thickne
the fractional area covered
and $g(H)$ is normalized such
some property which depends
ty within the region for whi

$$\bar{\phi} = \int_0^\infty \phi(H)g(H)dH \quad .$$

We shall refer to $\bar{\phi}$ as the
practice we usually conside
$g(H)$ is partitioned into n
mated as

$$\bar{\bar{\phi}} = \sum_{i=1}^{n} \Delta G_i \bar{\phi}_i$$

where $\bar{\phi}_i$ is the average val
$g_i \Delta H_i$. Since both ϕ and
use the notation

$$\langle \phi \rangle = \int_0^t \bar{\bar{\phi}}(t)dt$$

to denote quantities integra

5.4.2 Energy Exchange Over

To obtain regional est
must first know how each of
time. A detailed study of
conditions in the Central A
that the ice pack is predor
m and that the young ice is
tens to hundreds of meters
temperatures measured over
the turbulent heat fluxes
not strictly true, the ai
close to the lead surface
on the turbulent heat excha
the results obtained bel
perennial ice but will nc
growth of ice in the SSIZ
the growing ice.

ical distance of only
e and latent heat from
fluxes is latent heat
esult, ice production
Continual opening and
ice formation and new
rm ice cover composed
gh subject to similar
each of these differ-
winter rates of ice
atmosphere, and salt
s of magnitude larger
e. Although decreas-
hese rates can still
ce than over 3 m ice.
stinction between ice
large quantities of
ultimately affect the
ent estimates of heat
re based largely on
do not directly take
nd open water. For
n this omission is of
are sensitive to ice
ortion of the large
were composed of 99%
r ice production in
hly equal to that in
production for the
ted on the basis of
.

n dynamic and thermo-
n the amount of thin
hours to days, pro-
eat and mass balance
rgy fluxes. Because
ade by areas of thin
ce do not necessari-
aged heat and mass
s cannot be measured
ne, first, how each
with ice thickness
ven thickness. The
tegory is then found
that category times
. Summing over all

To quantify thickness variations within a particular region, Thorndike et al. (1975) introduced a probability density function g(H), called the ice thickness distribution, where $\int_{H_1}^{H_2} g(H)dH$ is the the fractional area covered by ice in the thickness range $H_1 \leq H < H_2$ and g(H) is normalized such that $\int_o^\infty g(H)dH = 1$. If we let ϕ be some property which depends on H, then the average of that property within the region for which g(H) is defined is given by

$$\bar{\phi} = \int_o^\infty \phi(H)g(H)dH \quad . \tag{5.31}$$

We shall refer to $\bar{\phi}$ as the regional or large scale average. In practice we usually consider discrete thickness categories. If g(H) is partitioned into n categories, eq. (5.31) can be approximated as

$$\bar{\phi} = \sum_{i=1}^{n} \Delta G_i \bar{\phi}_i \tag{5.32}$$

where $\bar{\phi}_i$ is the average value of ϕ in the i^{th} category and $\Delta G_i = g_i \Delta H_i$. Since both ϕ and g are in general functions of time, we use the notation

$$\langle\bar{\phi}\rangle = \int_o^t \bar{\phi}(t)dt$$

to denote quantities integrated over time.

5.4.2 Energy Exchange Over Young Sea Ice

To obtain regional estimates of the heat and mass balance, we must first know how each of the components vary with thickness and time. A detailed study of this problem has been carried out for conditions in the Central Arctic (Maykut, 1978). It was assumed that the ice pack is predominantly composed of ice thicker than 1 m and that the young ice is found mostly in narrow refrozen leads tens to hundreds of meters in width. It was also assumed that air temperatures measured over the thick ice could be used to estimate the turbulent heat fluxes over adjacent areas of thin ice. While not strictly true, the air mass modification which does occur close to the lead surface does not appear to have a large effect on the turbulent heat exchange (Vowinckel and Orvig, 1972). Thus the results obtained below describe conditions in regions of perennial ice but will not apply to the initial formation and growth of ice in the SSIZ where the boundary layer evolves with the growing ice.

With radiation data from Marshunova (1961; Table 1) and air temperatures derived from the data of Doronin (1963), a thin ice model similar to eqs. (5.27) and (5.28) was used to infer ice growth and energy fluxes over various thicknesses of ice throughout the year. Figure 24 shows predicted seasonal variations in surface temperature for different values of H. When the air was cold, T_o decreased rapidly with increasing H, reaching 50% of the perennial ice value at H = 10 cm and 90% of this value at H = 80 cm. The dependence of T_o on H became more subdued in the late spring and early fall when the ice was near the melting point.

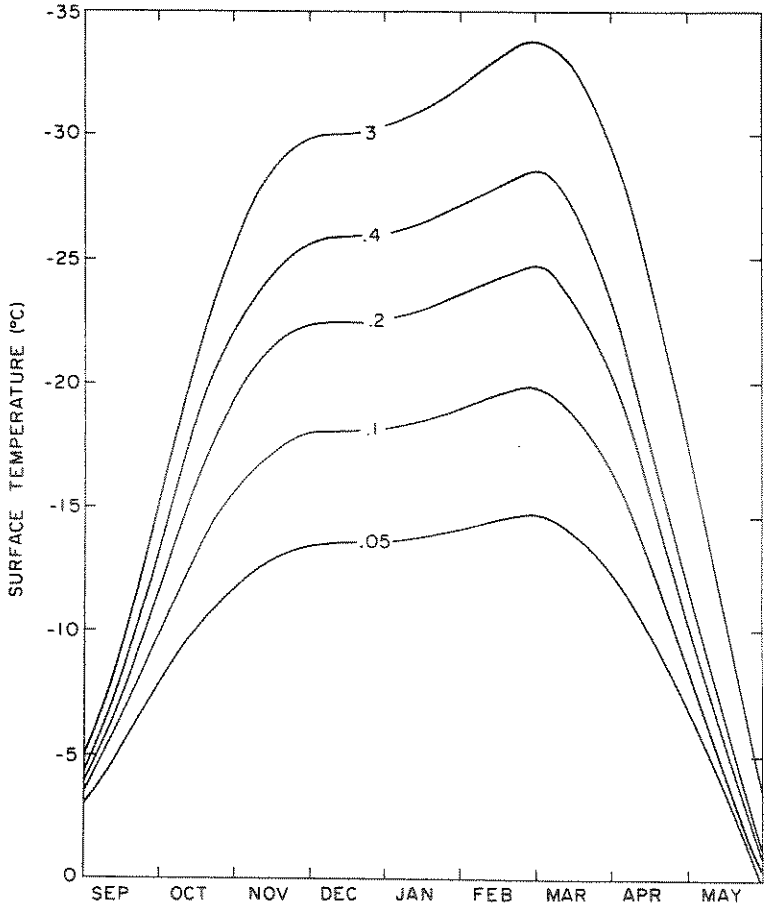

Fig. 24. Seasonal variations in surface temperatures over various thicknesses of ice in the Central Arctic. (After Maykut, 1978). Lines of constant ice thickness are given in meters.

Seasonal fluctuations
ice was thin, F_c domi
in the young ice wer
pheric forcing. Grov
using eq. (5.28). F_w
tions: (i) a constan
wave energy stored ir
Atlantic layer, and (i
of the shortwave ra
ocean. This is rough
tween the bottom of
thick ice.

Seasonal variati
Figures 26 and 27, w
Table 6. The result

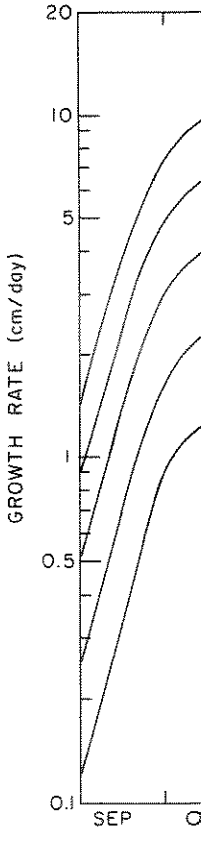

Fig. 25. Seasonal va
thickness (

1961; Table 1) and air
in (1963), a thin ice
was used to infer ice
nesses of ice through-
seasonal variations in
H. When the air was
H, reaching 50% of the
this value at H = 80
e subdued in the late
ar the melting point.

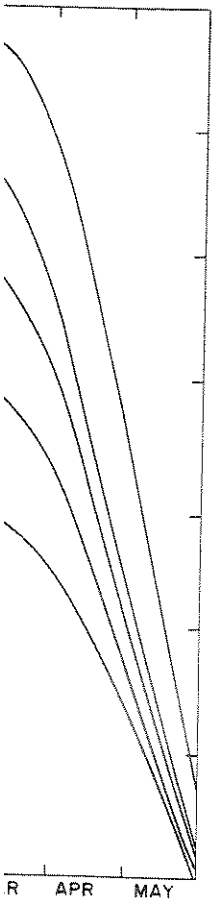

eratures over various
ctic. (After Maykut,
ckness are given in

Seasonal fluctuations in T_o increased as H increased. When the ice was thin, F_c dominated the heat balance so that temperatures in the young ice were only mildly sensitive to changes in atmospheric forcing. Growth rates (Figure 25) were obtained from T_o using eq. (5.28). F_w was assumed to be made up of two contributions: (i) a constant term (F_{wo} = 2 W m^{-2}) that includes shortwave energy stored in the upper ocean and any heat loss from the Atlantic layer, and (ii) a variable term that was taken to be 35% of the shortwave radiation transmitted through the ice to the ocean. This is roughly the amount of solar energy absorbed between the bottom of thin ice and the bottom of the surrounding thick ice.

Seasonal variations in the turbulent fluxes are shown in Figures 26 and 27, with a summary of all component presented in Table 6. The results show that F_s dominates the heat exchange

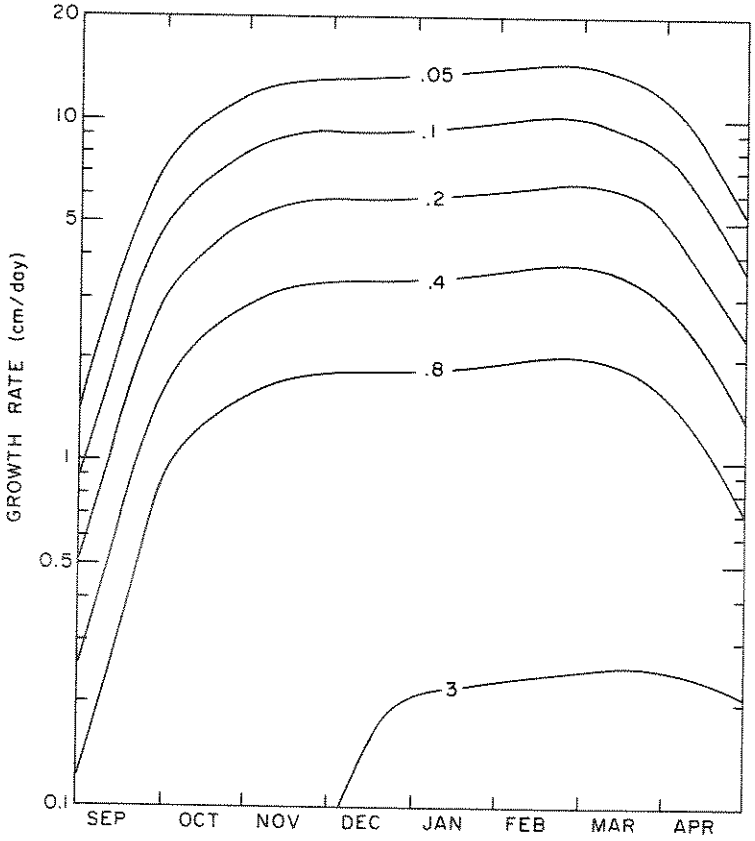

Fig. 25. Seasonal variations in growth rates as a function of ice thickness (cm). Note the logarithmic scale.

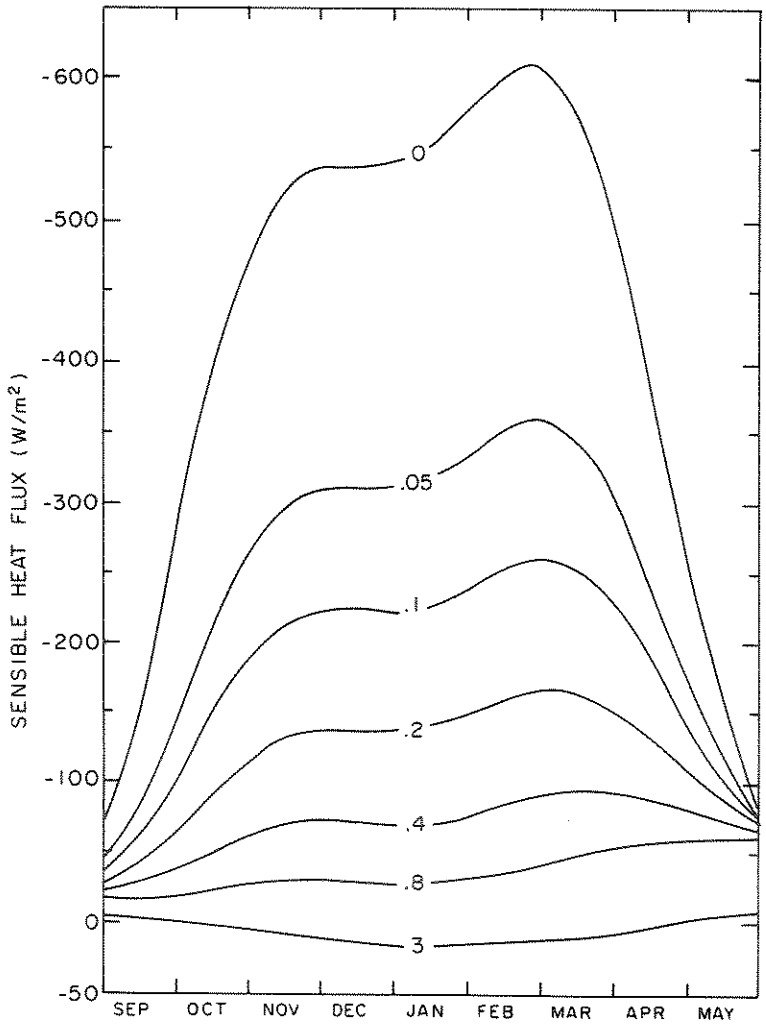

Fig. 26. Seasonal variation in the sensible heat flux as a function of ice thickness (m). (After Maykut, 1978.)

with the atmosphere over young ice. In early March, for example, F_s ranged from a small heat gain over the perennial ice to a loss over the open water that was about 3-1/2 times the total of the incident radiation fluxes. While F_e over open leads was comparable to the radiation fluxes throughout much of the winter, it decreased very rapidly with increasing H because of the steep decline in e_s below 0°C. Thus F_e (H > 20 cm) was of only secondary importance in the overall heat balance.

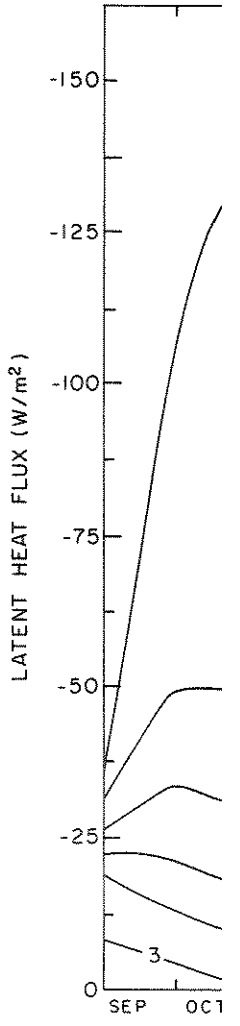

Fig. 27. Seasonal var
of ice thick

The results make
atmosphere (F_n) over
rate at which turbule
year ice F_s is compar
make an equal contrib
both supply heat to th
The calculations also
becomes insensitive to
saw in Figure 18, howe

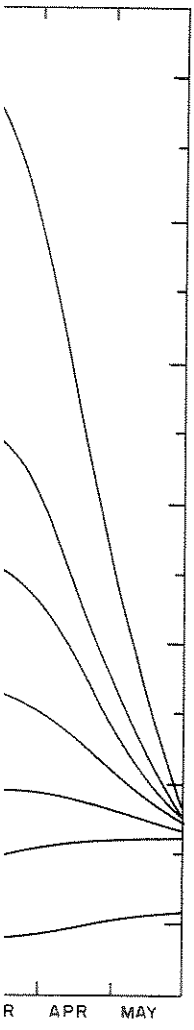

ıeat flux as a func-
ykut, 1978.)

March, for example,
ınnial ice to a loss
the total of the in-
leads was comparable
winter, it decreased
steep decline in e_s
secondary importance

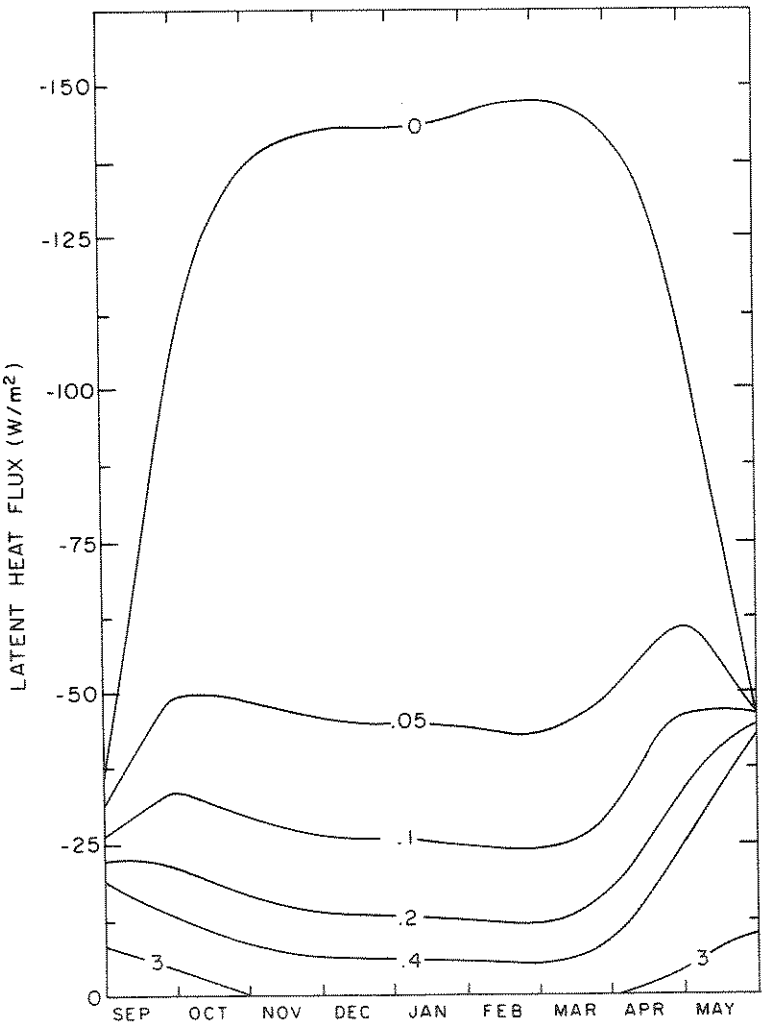

Fig. 27. Seasonal variation in the latent heat flux as a function of ice thickness (m). (After Maykut, 1978.)

The results make it clear that the net heat input to the atmosphere (F_n) over very thin ice is controlled primarily by the rate at which turbulent heat is transferred. Over thicker first year ice F_s is comparable to the net longwave radiation and both make an equal contribution to F_n. Over thick ice F_s and F_c must both supply heat to the surface to compensate for longwave losses. The calculations also demonstrate that the surface heat balance becomes insensitive to thickness once H exceeds 80-100 cm. As we saw in Figure 18, however, this is the range where the growth rates

Table 5.6. Heat balance over various ice thickness categories in the central Arctic. (After Maykut, 1978).

	Sep	Oct	Nov	Dec	Jan	Feb	Mar	Apr	May	June
					Open water					
Net shortwave radiation	89	24					7	83	209	281
Net longwave radiation	-28	-69	-114	-138	-142	-147	-149	-140	-98	-43
Sensible heat flux	-68	-259	-458	-540	-543	-575	-615	-520	-276	-33
Latent heat flux	-34	-108	-139	-145	-145	-147	-150	-144	-112	-31
Oceanic heat flux	130	436	711	823	830	869	914	804	486	107
					0.05 m					
Available shortwave energy*	60	16					5	56	141	189
Net longwave radiation	-22	-42	-70	-87	-91	-93	-93	-93	-76	-51
Sensible heat flux	-44	-142	-261	-311	-312	-334	-362	-313	-179	-74
Latent heat flux	-31	-50	-49	-47	-46	-45	-44	-51	-62	-47
Conductive heat flux	37	218	380	445	449	472	494	401	176	-17
					0.1 m					
Available shortwave energy	56	15					4	52	131	175
Net longwave radiation	-20	-33	-55	-69	-73	-75	-73	-77	-68	-50
Sensible heat flux	-36	-101	-186	-222	-222	-238	-262	-232	-143	-73
Latent heat flux	-27	-34	-30	-27	-26	-25	-24	-31	-47	-47
Conductive heat flux	27	153	271	318	321	338	355	288	127	-5
					0.2 m					
Available shortwave energy	53	14					4	49	124	166
Net longwave radiation	-19	-25	-41	-53	-57	-58	-55	-62	-61	-49
Sensible heat flux	-29	-64	-115	-137	-136	-147	-165	-154	-109	-68
Latent heat flux	-23	-22	-16	-14	-14	-13	-12	-17	-34	-46
Conductive heat flux	18	97	172	204	207	218	228	184	80	-3
					0.4 m					
Available shortwave energy	48	13					4	46	114	153
Net longwave radiation	-17	-19	-31	-41	-45	-45	-42	-51	-55	-47
Sensible heat flux	-22	-36	-62	-72	-70	-77	-91	-93	-82	-60
Latent heat flux	-19	-14	-9	-6	-6	-6	-5	-10	-26	-44
Conductive heat flux	10	56	102	119	121	128	134	108	49	-2
					0.8 m					
Available shortwave energy	45	12					3	42	104	140
Net longwave radiation	-16	-16	-24	-33	-37	-37	-34	-43	-51	-46
Sensible heat flux	-17	-18	-27	-30	-27	-31	-42	-53	-61	-54
Latent heat flux	-16	-9	-4	-3	-2	-2	-2	-5	-19	-39
Conductive heat flux	4	31	55	66	66	70	75	59	27	-1
					3.0 m					
Available shortwave energy	16	4					1	17	42	59
Net longwave radiation	-14	-12	-18	-26	-31	-29	-25	-32	-38	-35
Sensible heat flux	-5	0	6	11	17	16	12	9	-2	-8
Latent heat flux	-9	-4	0	0	0	0	0	0	-4	-10
Conductive heat flux	12	12	12	15	14	13	12	6	2	-6

Energy fluxes are given in watts per square meter and describe conditions on the first day of the month.

*$(1 - i_0)\ (1 - \alpha)F_r$.

become increasingly de
rather than just on H.

5.4.3 Ice Thickness Va

The second step i
and mass balance of the
by each thickness cate
Spatial variations on
(Wadhams and Horne, 19
to provide much data on
thin ice and open wate
heat and mass balance c
ly microwave, can provi
lution is still poor.

In the absence of
calculations offer a p
thickness distribution
growth data. The gov
(Thorndike et al., 1975

$$\frac{\partial g}{\partial t} = -\frac{\partial}{\partial H}(fg) - g$$

where f(H,t) is the g
field of the ice, and
scribes how thin ice i
on the right-hand si
g(H,t) of: (i) thermod
traction of the region
ice into or out of the
caused by convergence
from the motion of d
f(H,t) can be calculate
dynamic ice growth mod
there are some difficu
the model parameterize
processes, and we have
or predictions made b
large scale strain fie
of points several hund
that there exists a
scale strains and the
relationship is not ba
ably not only a funct
small scale random mot
role these random moti
be established.

ıickness categories in
t, 1978).

eb	Mar	Apr	May	June
r				
	7	83	209	281
47	-149	-140	-98	-43
75	-615	-520	-276	-33
47	-150	-144	-112	-31
59	914	804	486	107
	5	56	141	189
33	-93	-93	-76	-51
34	-362	-313	-179	-74
35	-44	-51	-62	-47
72	494	401	176	-17
	4	52	131	175
75	-73	-77	-68	-50
38	-262	-232	-143	-73
35	-24	-31	-47	-47
48	355	288	127	-5
	4	49	124	166
8	-55	-62	-61	-49
7	-165	-154	-109	-68
3	-12	-17	-34	-46
8	228	184	80	-3
	4	46	114	153
5	-42	-51	-55	-47
7	-91	-93	-82	-60
6	-5	-10	-26	-44
8	134	108	49	-2
	3	42	104	140
7	-34	-43	-51	-46
1	-42	-53	-61	-54
2	-2	-5	-19	-39
0	75	59	27	-1
	1	17	42	59
9	-25	-32	-38	-35
6	12	9	-2	-8
0	0	0	-4	-10
3	12	6	2	-6

onditions on the first day of

become increasingly dependent on the thermal history of the ice rather than just on H.

5.4.3 Ice Thickness Variations

The second step in obtaining regional estimates of the heat and mass balance of the ice pack is to find out the area covered by each thickness category and how this area changes with time. Spatial variations on H can be measured with submarine sonar (Wadhams and Horne, 1978), but the coverage is too limited in time to provide much data on temporal variations in the distribution of thin ice and open water, information of particular concern in the heat and mass balance calculations. Satellite imagery, particularly microwave, can provide frequent coverage but the thickness resolution is still poor.

In the absence of suitable observational methods, theoretical calculations offer a possible way to estimate changes in the ice thickness distribution on a routine basis from strain and ice growth data. The governing equation for g(H,t) can be written (Thorndike et al., 1975)

$$\frac{\partial g}{\partial t} = -\frac{\partial}{\partial H}(fg) - g \operatorname{div} \vec{V} - \vec{V} \cdot \bar{\nabla} g + \psi(H,\vec{V}) \qquad (5.33)$$

where f(H,t) is the growth rate of the ice, $\vec{V}$ is the velocity field of the ice, and ψ is the redistribution function which describes how thin ice is ridged into pressure ice. The four terms on the right-hand side of eq. (5.33) describe the effects on g(H,t) of: (i) thermodynamic changes in H, (ii) expansion or contraction of the region for which g is defined, (iii) advection of ice into or out of the region, and (iv) mechanical changes in H caused by convergence or shear. Information on $\vec{V}$ is available from the motion of drifting stations and unmanned buoys, while f(H,t) can be calculated from the heat balance data using a thermodynamic ice growth model. Although eq. (5.33) is quite general, there are some difficulties with its application. In particular, the model parameterizes a number of complex and poorly understood processes, and we have no real way to test these parameterizations or predictions made by the model. Another problem involves the large scale strain field which must be calculated from the movement of points several hundreds of kilometers apart. We have assumed that there exists a functional relationship between these large scale strains and the local opening and closing of leads, but this relationship is not based on measurements. Local opening is probably not only a function of the large scale strain but also of small scale random motions unrelated to this strain. How large a role these random motions play in the local deformation is yet to be established.

In spite of these uncertainities, numerical experiments with the thickness distribution model (Thorndike et al., 1975) showed that predictions were consistent with what is known about g(H,t) in the Central Arctic. It was therefore decided to utilize the model for estimating regional energy fluxes and rates of ice production. Ice thickness distributions were calculated for three different sets of strain data taken from drifting stations in the Central Arctic. The first two sets were obtained during the Arctic Ice Dynamics Joint Experiment (AIDJEX) in the Beaufort Sea and include year-long strain histories from the four manned camps and from the extensive data buoy network (Thorndike and Cheung, 1977; Colony, 1978). The third set was derived from the motions of Ice Stations T-3, ARLIS II and NP-10 during a 2-year period between 1962 and 1964. These data differ markedly in terms of space scales, time scales, and measurement accuracy. Because they contain the least smoothing and were constructed from the most accurate positions, strains from the AIDJEX manned camp array probably provide the best measure of deformational activity within the ice pack. The thickness distribution based on these strains is shown in Figure 28. The amount of ice in the thinnest category averaged only .2-.3% during the winter, essentially reflecting strains which occurred during the preceding day. The total amount of young (H<80 cm) ice varied from 4-6% during this period. Satellite data (Ahlnas and Wendler, 1977) indicate that "young ice" coverage in the Beaufort Sea averaged at least 15% in March 1973 and 6% in March 1974. Submarine data (Wittmann and Schule, 1966) indicate that "young ice" comprises 8-12% of the ice pack between January and May. The maximum thickness of the young ice included in these estimates is unknown, but seems unlikely to exceed 80 cm. The young ice estimates in Figure 28 may thus be somewhat conservative during winter and early spring. The substantial increase in the amount of young ice in May appears to reflect persistent divergence occurring during April and May. The large amount of open water in August results from the melting of young ice and from divergence of the array during July and August. While the 17% figure seems excessive, an aerial mosaic of the array made during mid-August revealed an average of 12-15% open water (R. T. Hall, personal communication). In light of this evidence, the calculated summer values may not be unreasonable.

5.4.4 Regional Fluxes

Using the incident radiation fluxes of Marshunova (1961) and the turbulent fluxes of Doronin (1963), area weighted averages of all thickness dependent quantities were calculated at 6 hour intervals throughout the year for the AIDJEX manned camp array, then integrated over time to obtain the monthly flux totals shown in Table 7. Because of their weak dependence on H, heat flux contributions from the thicker ice were collected into a single category (0.8-∞m). The results show that effects of g(H) on the individual

Fig. 28. Ice thicknes
AIDJEX manned

radiative fluxes are s
(n relation to the net
radiation by young ic
losses 3-6% above tho
negligible. The low
summer absorption of s
the annual net radiati
large as the value ov
energy was absorbed
absorbed by the water
(T_w) at or above the
in the water, i.e.,

$$I_{ow} = (1 - \alpha_w)F_r$$

ical experiments with
et al., 1975) showed
is known about g(H,t)
cided to utilize the
and rates of ice pro-
calculated for three
fting stations in the
obtained during the
in the Beaufort Sea
he four manned camps
Thorndike and Cheung,
ved from the motions
ring a 2-year period
arkedly in terms of
curacy. Because they
ucted from the most
X manned camp array
ional activity within
ised on these strains
he thinnest category
sentially reflecting
y. The total amount
this period. Satel-
te that "young ice"
st 15% in March 1973
nn and Schule, 1966)
the ice pack between
e young ice included
cely to exceed 80 cm.
be somewhat conserva-
stantial increase in
ect persistent diver-
large amount of open
young ice and from
ust. While the 17%
he array made during
water (R. T. Hall,
dence, the calculat-

arshunova (1961) and
veighted averages of
lated at 6 hour in-
ied camp array, then
lux totals shown in
l, heat flux contri-
to a single category
l) on the individual

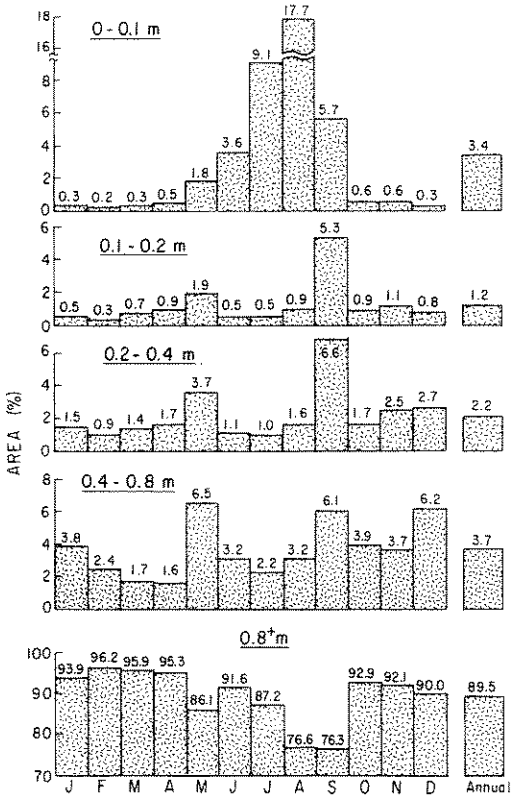

. 28. Ice thickness distribution in the region defined by the AIDJEX manned camps. (After Maykut, 1982.)

diative fluxes are small on a percentage basis, but significant relation to the net heat balance. Greater emission of longwave diation by young ice during the winter increased net longwave ses 3-6% above those over thick ice; summer differences were ligible. The low albedo of leads and thin ice increased the ner absorption of shortwave radiation by 10-20%. As a result annual net radiation balance for the region was over twice as e as the value over perennial ice. Most of this additional ergy was absorbed in the water. Part of the solar radiation orbed by the water is needed to maintain the water temperature at or above the freezing point. The remainder, I_{ow}, is stored the water, i.e.,

$$I_{ow} = (1 - \alpha_w)F_r + F_L - \sigma T_w^4 + F_s + F_e \quad .$$

Table 5.7. Area weighted heat flux (MJ m^{-2} mo^{-1}) over the AIDJEX manned array. (After Maykut, 1982.)

	Thickness category	Jan	Feb	Mar	Apr	May	Jun	Jul	Aug	Sep	Oct	Nov	Dec	Annual
Net radiation	0-0.1	-0.6	-0.4	-0.6	0.6	7.4	21.6	44.4	46.6	5.5	-0.7	-1.2	-0.8	121.8
	0.1-0.2	-0.8	-0.5	-0.8	1.4	6.7	2.1	1.5	1.7	3.5	-0.7	-1.6	-1.3	11.2
	0.2-0.4	-2.0	-1.1	-1.1	2.7	11.7	4.4	3.1	2.8	2.9	-0.9	-2.7	-3.3	16.5
	0.4-0.8	-4.1	-2.4	-0.9	1.9	18.0	10.8	5.9	5.0	2.1	-1.3	-3.3	-5.9	25.8
	0.8-∞	-74.2	-65.2	-50.2	-10.9	48.5	85.6	181.8	86.5	-1.7	-30.8	-55.4	-60.9	53.1
	TOTAL	-81.7	-69.6	-53.6	-4.3	92.3	124.5	236.7	142.6	12.3	-34.4	-64.2	-72.2	228.4
	3 m	-79.0	-67.8	-52.4	-10.8	56.5	94.3	207.9	111.2	-1.8	-33.1	-60.2	-67.6	97.2
Energy excess in leads $\langle I_\ell \rangle$				0.3	2.4	10.6	10.6	18.8	24.9	6.4	0.3			74.3
Energy absorbed below ice $\langle I_w \rangle$				0.5	4.1	17.2	17.4	29.9	29.3	8.0	0.3			106.7
Radiation stored in ice $\langle I_i \rangle$								64.0	31.3					95.3
Sensible heat flux $\langle F_s \rangle$	0-0.1	-2.1	-1.4	-2.9	-2.9	-4.7	-1.0	-1.2	-0.7	-8.1	-2.9	-4.4	-2.7	-35.0
	0.1-0.2	-2.3	-1.6	-3.4	-3.2	-3.5	-0.2	-0.1	-0.2	-5.0	-2.6	-4.7	-3.8	-30.6
	0.2-0.4	-3.9	-2.6	-4.4	-4.0	-5.7	-0.6	-0.1	-0.3	-5.0	-2.7	-6.3	-7.4	-43.0
	0.4-0.8	-4.7	-3.6	-2.8	-2.6	-9.3	-1.9	-0.3	-0.6	-3.1	-3.0	-4.7	-8.2	-44.8
	0.8-∞	43.7	32.8	27.8	11.1	-13.4	-15.2	-11.8	-12.0	-5.7	4.6	20.5	30.9	113.3
	TOTAL	30.7	23.6	14.3	-1.6	-36.6	-18.9	-13.5	-13.8	-26.9	-6.6	0.4	8.8	-40.1
	3 m	46.5	34.1	29.0	11.3	-15.6	-16.7	-13.6	-15.7	-7.5	4.9	22.3	34.3	113.3
Latent heat flux $\langle F_e \rangle$	0-0.1	-0.3	-0.2	-0.4	-0.7	-2.2	-1.3	-2.5	-3.1	-4.8	-0.8	-0.8	-0.4	-17.5
	0.1-0.2	-0.3	-0.2	-0.3	-0.7	-1.5	-0.2	-0.1	-0.3	-2.9	-0.6	-0.6	-0.4	-8.1
	0.2-0.4	-0.4	-0.2	-0.4	-0.8	-2.5	-0.6	-0.3	-0.5	-2.7	-0.6	-0.7	-0.8	-10.5
	0.4-0.8	-0.5	-0.3	-0.2	-0.5	-4.3	-1.8	-0.6	-0.9	-1.8	-0.9	-0.5	-0.8	-13.1
	0.8-∞	0.0	0.0	0.0	-3.2	-16.2	-26.1	-24.0	-20.5	-12.7	-7.3	-0.1	0.0	-110.1
	TOTAL	-1.5	-0.9	-1.3	-5.9	-26.7	-30.0	-27.5	-25.3	-24.9	-10.2	-2.7	-2.4	-159.3
	3 m	0.0	0.0	0.0	-3.5	-18.8	-28.4	-27.5	-26.7	-16.8	-7.9	-0.1	0.0	-129.7
Conductive heat flux $\langle F_c \rangle$	0-0.1	3.1	2.0	4.1	4.1	6.1	0.1	0.0	3.3	13.7	4.6	6.4	3.9	51.4
	0.1-0.2	3.4	2.3	4.7	4.2	3.6	0.0	0.0	0.1	8.1	3.9	6.7	5.5	42.5
	0.2-0.4	6.3	3.9	6.2	4.6	4.1	0.0	0.0	0.0	7.8	4.4	9.8	11.4	58.5
	0.4-0.8	9.3	6.2	4.2	2.3	3.6	0.0	0.0	0.0	4.4	5.5	8.5	14.9	58.9
	0.8-∞	30.6	32.4	22.4	3.1	-19.0	-4.5	0.0	0.0	20.1	33.5	35.0	29.9	183.5
	TOTAL	52.7	46.8	41.6	18.3	-1.6	-4.4	0.0	3.4	54.1	51.9	66.4	65.6	394.8
	3 m	32.5	33.7	23.4	3.0	-22.1	-5.0	0.0	0.0	26.1	36.1	38.0	33.3	199.0

Let us now resolve I_c shortwave radiation ab rounding ice, and I_ℓ = absorbed in the upper the atmosphere at the tween the ice and wat horizontal, while stat downward mixing of I_ℓ. as the sum of three te

$$\langle I_o \rangle = \langle I_i \rangle + \langle I_w$$

where $\langle I_i \rangle$ = the amou slowly returns to the during the fall, but of the ice pack throu floe edges. The calc entirely into I_w and I

The amount of h variations in ice thic additional heat was fluxes. Figure 29a sh the thickness categori gorty (0-0.1 m) did n intermediate thickness sible for over half t tween regional and 3 29b) in conjunction wi

Regional ice pro tributions from young of ice produced in th .154 m in thickness co tion for the entire r mass balance expected ice accounted for ess extremely large growth m category made up production, reflecting the winter. Seasona and are compared with though $\langle f \rangle$ was 2-3 t largest differences stored during the sum ing most of the ocean tion; in thin ice co than F_w and ice growt water created during of ice production dur

Heat Flux	0.4–0.8	-0.5	-0.3	-0.2	-0.5	-4.3	-1.8	-0.6	-0.9	-1.8	-0.9	-0.5	-0.8	-13.1	
$\langle F_e \rangle$	0.8– ∞	0.0	0.0	0.0	-3.2	-16.2	-26.1	-24.0	-20.5	-12.7	-7.3	-0.1	0.0	-110.1	
	TOTAL	-1.5	-0.9	-1.3	-5.9	-26.7	-30.0	-27.5	-25.3	-24.9	-10.2	-2.7	-2.4	-159.3	
	3 m	0.0	0.0	0.0	-3.5	-18.8	-28.4	-27.5	-26.7	-16.8	-7.9	-0.1	0.0	-129.7	
	0–0.1	3.1	2.0	4.1	4.1	6.1	0.1	0.0	3.3	13.7	4.6	6.4	3.9	51.4	
	0.1–0.2	3.4	2.3	4.7	4.2	3.6	0.0	0.0	0.1	8.1	3.9	6.7	5.5	42.5	
Conductive	0.2–0.4	6.3	3.9	6.2	4.6	4.1	0.0	0.0	0.0	7.8	4.4	9.8	11.4	58.5	
heat flux	0.4–0.8	9.3	6.2	4.2	2.3	3.6	0.0	0.0	0.0	4.4	5.5	8.5	14.9	58.9	
$\langle F_c \rangle$	0.8– ∞	30.6	32.4	22.4	3.1	-19.0	-4.5	0.0	0.0	20.1	33.5	35.0	29.9	183.5	
	TOTAL	52.7	46.8	41.6	18.3	-1.6	-4.4	0.0	3.4	54.1	51.9	66.4	65.6	394.8	
	3 m	32.5	33.7	23.4	3.0	-22.1	-5.0	0.0	0.0	26.1	36.1	38.0	33.3	199.0	

Let us now resolve I_{ow} into two components: I_w = the amount of shortwave radiation absorbed beneath the bottom (3 m) of the surrounding ice, and I_ℓ = the difference between the shortwave energy absorbed in the upper 3 m of the leads and the net heat loss to the atmosphere at the surface of the leads. Relative motions between the ice and water tend to distribute I_w uniformly in the horizontal, while stability of the water in summer leads inhibits downward mixing of I_ℓ. Regional values of I_o can thus be expressed as the sum of three terms

$$\langle I_o \rangle = \langle I_i \rangle + \langle I_w \rangle + \langle I_\ell \rangle$$

where $\langle I_i \rangle$ = the amount of solar energy stored within the ice. I_i slowly returns to the atmosphere as the brine pockets freezing during the fall, but I_w and I_ℓ primarily affect the mass balance of the ice pack through bottom ablation and lateral melting on floe edges. The calculated increase in net radiation went almost entirely into I_w and I_ℓ.

The amount of heat conducted to the surface doubled when variations in ice thickness were taken into account. Most of this additional heat was lost to the atmosphere via the turbulent fluxes. Figure 29a shows total turbulent heat losses from each of the thickness categories. It is notable that the ope water category (0–0.1 m) did not dominate the balance, rather it was the intermediate thicknesses (0.2–0.8 m) of young ice that were responsible for over half the total loss. The greatest differences between regional and 3 m values occurred during the fall (Figure 29b) in conjunction with the rapid ice production.

Regional ice production $\langle f \rangle$ was dramatically larger when contributions from young ice were considered (Figure 30a). The mass of ice produced in the 0–0.1 m category was equivalent to a layer .154 m in thickness covering the entire array. Annual ice production for the entire region totaled .886 m, in contrast to the zero mass balance expected for 3 m ice. Growth in areas of first year ice accounted for essentially all the ice production. Despite the extremely large growth rates in new leads, ice growth in the 0–0.1 m category made up only about 16% of the total first year ice production, reflecting the small area occupied by open water during the winter. Seasonal variations in $\langle f \rangle$ are shown in Figure 30b, and are compared with the corresponding values for 3 m ice. Although $\langle f \rangle$ was 2–3 times the 3 m values during the winter, the largest differences occurred in the fall. In thick ice heat stored during the summer retarded conduction at the bottom, allowing most of the oceanic heat flux to go directly into bottom ablation; in thin ice conductive fluxes in the ice were much larger than F_w and ice growth was rapid. Ice formation in areas of open water created during the summer was responsible for the large rates of ice production during the fall.

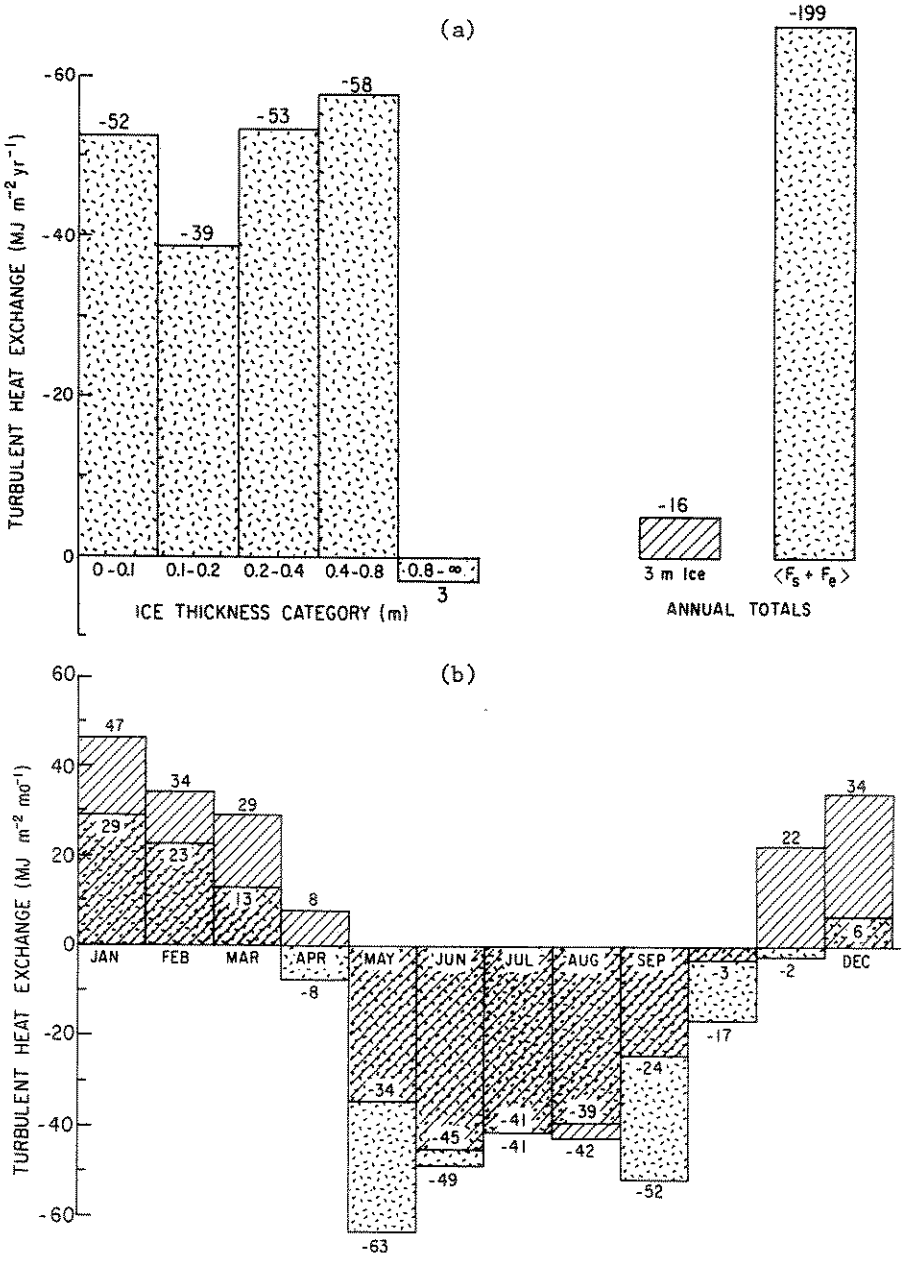

Fig. 29. Total turbulent heat exchange [F_s + F_e] over the AIDJEX manned array. (a) Annual totals in each thickness category. (b) Monthly totals obtained by taking into account ice thickness variations (stippled) and by assuming a uniform 3 m ice cover (cross-hatched). (After Maykut, 1982.)

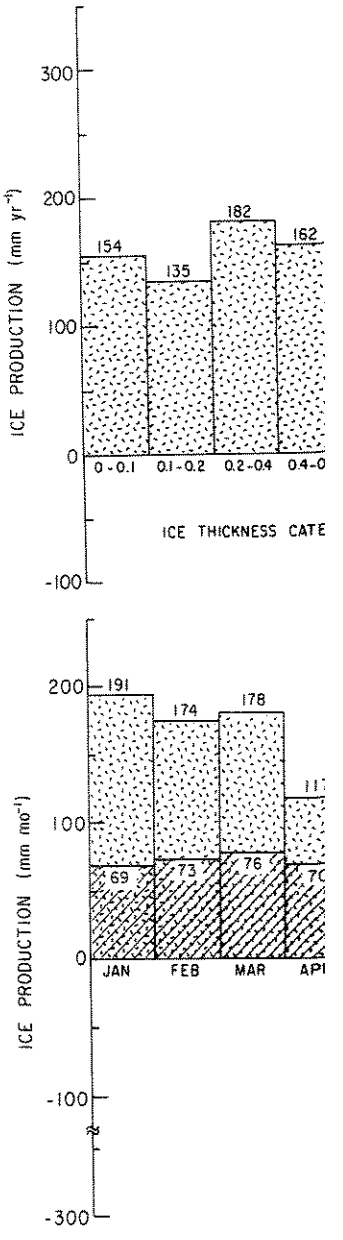

Fig. 30. Ice production totals in each obtained by tal (stippled) and (cross-hatched)

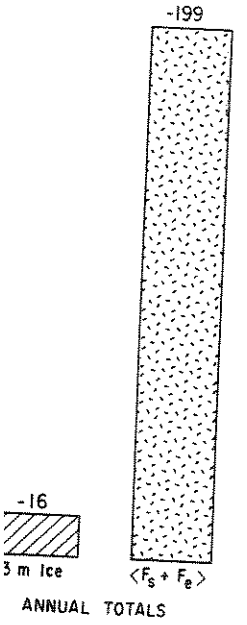

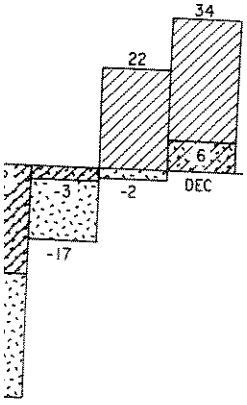

e] over the AIDJEX
ch thickness cate-
taking into account
and by assuming a
). (After Maykut,

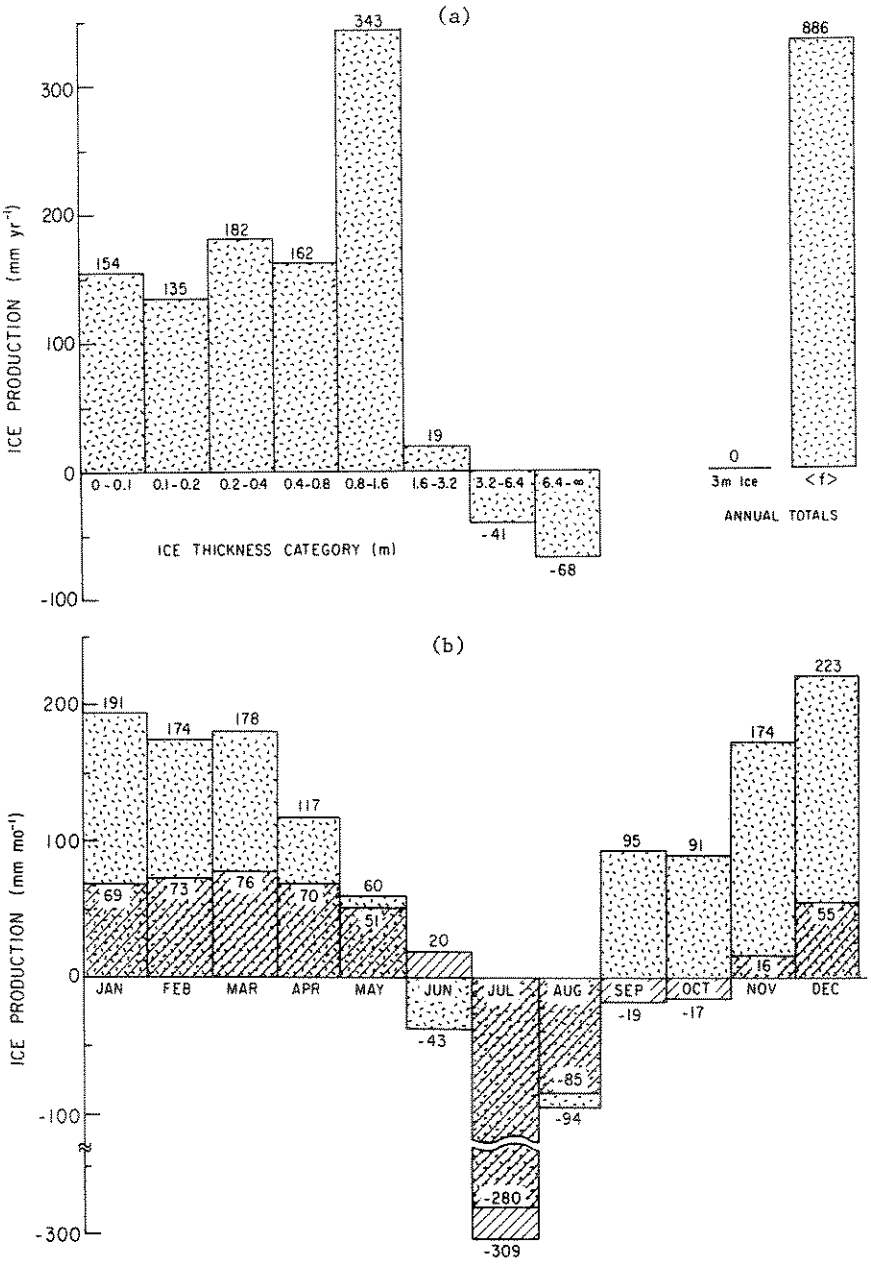

Fig. 30. Ice production in the AIDJEX manned array. (a) Annual totals in each thickness category. (b) Monthly totals obtained by taking into account ice thickness variations (stippled) and by assuming a uniform 3 m ice cover (cross-hatched). (After Maykut, 1982).

Given the uncertainties in how well large scale strains represent local deformation, it is of particular interest to examine how the regional fluxes respond to different strains and strain statistics. Table 8 compares the effects of the three different strain histories mentioned previously. Annual net radiation totals varied by about 25% and were 2-1/2 to 3 times larger than would be expected if there were no strains (i.e., if all the ice were in thermodynamic equilibrium). Net radiation was largest in the 1962/63 T-3 triangle, despite having the smallest change in area during the year. This case did, however, average roughly 5% more open water during the summer as a result of substantial opening in June and July, and hence absorbed the most shortwave radiation. It might be expected that fall ice production for this case would be greatest due to the large amount of open water. In fact, <f> for 1962/63 was the least of any of the four cases studied, owing to strong convergence between August and November which closed up the open water and ridged the thin ice.

Table 5.8. Effect of different strain histories on regional totals. (After Maykut, 1982.)

	AIDJEX Manned Camps	AIDJEX Buoys	T-3 Triangle (1962/63)	T-3 Triangle (1963/64)	No Strains
Net radiation ($MJ\ m^{-2}\ year^{-1}$)	228	267	292	237	97
Solar radiation absorbed in leads ($MJ\ m^{-2}\ year^{-1}$)	74	86	114	80	
Solar radiation absorbed beneath ice ($MJ\ m^{-2}\ year^{-1}$)	107	128	160	119	
Turbulent heat exchange ($MJ\ m^{-2}\ year^{-1}$)	-199	-190	-155	-202	-16
Conductive heat flux (MJ m-2 $year^{-1}$)	395	381	349	400	199
Salt flux ($kg\ m^{-2}\ year^{-1}$)	12.7	14.8	10.2	19.2	-4.3
Ice production ($m\ year^{-1}$)	.89	.95	.71	1.16	0
Change in area of strain array (% per year)	18	17	9	50	

THE SURFACE HEAT AND MA

The most anomalous
which underwent a 50% i
sistent divergence obs
different flow regimes
Drift Stream, while T-
strains are not typica
opportunity to study t
an extreme situation.
was not greatly affect
net radiation, $\langle F_s \rangle$,
departures from the ot
overall level of diver
in excess of 1.1 m year
ice could not quite ke
for increased diverge
gests that the amount
very sensitive to var
the other hand, produc
is no quick way for th
in mass.

Ice strains typi
vergence over periods
the production of open
mation of existing ice
divergence and the hea
gest that the short te
to the regional therm
fact, other numerical
reproduce monthly hea
strain histories posse
balance, however, appe
of the strain componen

One of the least
and mass balance of th
in the ocean. Our
energy enters the upp
how this energy migh
of I_w and I_ℓ separat
ward into leads an
beneath the ice, we a
primarily into F_w ar
potentially available
ted, I_ℓ ranged betwe
energy is sufficient
However, the situatio
changing stratificati
regarding the relative
as in summer leads.

large scale strains rep-
ılar interest to examine
rent strains and strain
of the three different
Annual net radiation
to 3 times larger than
s (i.e., if all the ice
adiation was largest in
the smallest change in
ver, average roughly 5%
result of substantial
bed the most shortwave
ice production for this
unt of open water. In
any of the four cases
en August and November
e thin ice.

istories on regional

T-3 Triangle (1963/64)	No Strains
237	97
80	
119	
-202	-16
400	199
19.2	-4.3
1.16	0
50	

The most anomalous case was that of the 1963/64 T-3 triangle which underwent a 50% increase in area during the year. The persistent divergence observed arose because the array spanned two different flow regimes -- NP-10 and ARLIS II were in the Transpolar Drift Stream, while T-3 was in the Beaufort Gyre. Although such strains are not typical of the arctic ice pack, they offer an opportunity to study the response of the heat and mass balance to an extreme situation. Surprisingly, the regional heat exchange was not greatly affected by the large total divergence. Neither net radiation, $\langle F_s \rangle$, $\langle F_e \rangle$, nor $\langle F_c \rangle$ exhibited any consistent departures from the other cases. Only $\langle f \rangle$ was correlated with the overall level of divergence. However, in spite of ice production in excess of 1.1 m year^{-1}, $\bar{H}$ decreased by 0.3 m as the thermodynamics could not quite keep pace with the divergence. The tendency for increased divergence to cause increased ice production suggests that the amount of ice in the Arctic Basin is probably not very sensitive to variations in ice export. Net convergence, on the other hand, produces an immediate increase in $\bar{H}$ because there is no quick way for the thermodynamics to balance out the increase in mass.

Ice strains typically alternate between divergence and convergence over periods of days, so there are continual changes in the production of open water, the growth of new ice, and the deformation of existing ice. The weak correlation between the average divergence and the heat flux totals (both monthly and annual) suggest that the short term variations in strain are more important to the regional thermodynamics than the long term averages. In fact, other numerical experiments indicate that it is possible to reproduce monthly heat flux totals fairly well with different strain histories possessing similar variance. Effects on the mass balance, however, appear more closely related to the time average of the strain components.

One of the least understood aspects of the large scale heat and mass balance of the ice pack is the role played by heat stored in the ocean. Our results show that a great deal of shortwave energy enters the upper ocean through summer leads. To estimate how this energy might interact with the ice cover, we kept track of I_w and I_ℓ separately. Although part of I_w can be conducted upward into leads and occasional lead closures can transport I_ℓ beneath the ice, we assume as a first approximation that I_w goes primarily into F_w and that I_ℓ represents the amount of energy potentially available for lateral melting. In the four years studied, I_ℓ ranged between 75 and 115 MJ m^{-2} year^{-1}. This amount of energy is sufficient to decrease the ice concentration by 6-10%. However, the situation is complicated by ice movement, wind mixing, changing stratification of the surface waters, and uncertainities regarding the relative importance of various heat transfer processes in summer leads. At this point we have no reliable way to

estimate what fraction of $\langle I_\ell \rangle$ actually goes into lateral melting. While it seems evident that lateral melting is an important element in the summer mass balance, particularly in the marginal ice zone, systematic studies to define and quantify the dominant melt processes are needed before adequate models can be developed.

Shortwave radiation absorbed beneath the ice (I_w) was about 1.5-2.0 times as large as that needed to maintain a uniform 3 m thick ice cover. Some of this energy may escape to the atmosphere through leads, but most must ultimately interact directly with the ice. If F_w included both this energy and the heat lost from the Atlantic layer, theoretical calculations predict an equilibrium thickness of less than 1 m. Unless there are substantial energy sinks associated with the nonuniform nature of the ice cover, this suggests that little heat from the Atlantic layer reaches the ice, at least in the Central Arctic. Even if we neglect possible contributions from the Atlantic water, there appears to be a surplus of energy beneath the ice. A probable sink for much of this heat is the melting of ice eroded from pressure ridge keels. Measurements made on a pair of 9-12 m ridges over a three month period in the summer of 1975 (Rigby and Hanson, 1976) showed thickness changes of 1-4 m, apparently due to both melting and mechanical erosion. Presumably much of the ice eroded from the keels would spread out under the ice and be eventually melted by heat contained in the water. If we assume an effective F_w of 2.0-2.6 W m^{-2} beneath level ice, then the 3.4 W m^{-2} calculated for $\langle I_w \rangle$ in the AIDJEX manned triangle requires a net annual bottom ablation of 0.85-1.25 m from ice over 6 m in thickness, an amount consistent with the 1.5 m average observed by Rigby and Hanson.

These calculations show that thin ice and open water resulting from differential ice movement cause large-scale interactions between the ocean and atmosphere to be much more vigorous than would be expected on the basis of drifting station data. Dynamic effects during the winter are confined largely to increased ice production, salt flux to the ocean and sensible heat input to the atmosphere; during the summer dynamics strongly influence the interaction of shortwave radiation with the ice and ocean. Despite the numerous uncertainties, the results described above appear to provide a reasonable picture of how dynamic processes and thickness variations affect the heat and mass balance in regions of perennial ice.

ACKNOWLEDGMENTS

Special thanks go to Steve Warren and Norbert Untersteiner for many helpful comments and suggestions during the preparation of the manuscript. This review was made possible by support from the Office of Naval Research, Arctic Program, under Contract N00014-76-C-0234.

REFERENCES

Aagaard, K. and P. Gr
budgets for the
3821-3827.
Aagaard, K., L. K. Coac
of the Arctic Ocean
Ackley, S. F. (1981) Sea
Sea using drifting
Change (I. Allison
131, p. 177-191.
Ahlnas, K. and G. Wend
early spring viewed
Allison, I. (1981) Antar
In Sea Level Ice ar
Washington, D.C., P
Anderson, D. L. (1961)
1170-1172.
Anderson, D. L. (1958)
In Arctic Sea Ice,
D.C., National Rese
Andreas, E. L. (1980)
arctic leads. Mon.
Andreas, E. L. and S. F.
tion seasons of th
Sci., 39: 440-447.
Arnold, K. C. (1961) An
the melting of i
Geology of the Arc
Ontario, Canada, Vo
Badgley, F. I. (1966)
Ocean. In Proceed
and Atmospheric (
Corp., Santa Monica
Banke, E. G., S. D. Sm
cients at AIDJEX.
Pritchard, Ed.),
Washington, p. 430-
Bilello, M. A. (1961)
the Canadian Arcti
Brooks, C. E. P. (1949
New York, 395 p.
Budyko, M. I. (1966)
Symposium on the A
tion (J. O. Fle
California, RM-523
Budyko, M. I. (1974) Cl
Series 18. Academ

es into lateral melting.
g is an important ele-
rly in the marginal ice
ıtify the dominant melt
can be developed.

the ice (I_w) was about
maintain a uniform 3 m
scape to the atmosphere
eract directly with the
the heat lost from the
predict an equilibrium
are substantial energy
of the ice cover, this
layer reaches the ice,
neglect possible con-
ppears to be a surplus
for much of this heat
ridge keels. Measure-
three month period in
976) showed thickness
ıelting and mechanical
from the keels would
melted by heat con-
tive F_w of 2.0-2.6 W
alculated for $\langle I_w \rangle$ in
nnual bottom ablation
is, an amount consist-
ınd Hanson.

nd open water result-
ge-scale interactions
h more vigorous than
cation data. Dynamic
ely to increased ice
le heat input to the
ongly influence the
e and ocean. Despite
ibed above appear to
processes and thick-
ılance in regions of

Norbert Untersteiner
ing the preparation
ible by support from
am, under Contract

REFERENCES

Aagaard, K. and P. Greisman (1975) Toward new mass and heat budgets for the Arctic Ocean. J. Geophys. Res., 80: 3821-3827.

Aagaard, K., L. K. Coachman and E. Carmack (1981) On the halocline of the Arctic Ocean. Deep Sea Res., 28: 529-545.

Ackley, S. F. (1981) Sea-ice-atmosphere interactions in the Weddell Sea using drifting buoys. In Sea Level Ice and Climatic Change (I. Allison, Ed.), IAHS, Washington, D.C., Publication 131, p. 177-191.

Ahlnas, K. and G. Wendler (1977) Arctic sea ice conditions in early spring viewed by satellite. Arct. Alp. Res., 9: 61-72.

Allison, I. (1981) Antarctica sea ice growth and oceanic heat flux. In Sea Level Ice and Climatic Change (I. Allison, Ed.), IAHS, Washington, D.C., Publication 131, p. 161-170.

Anderson, D. L. (1961) Growth rate of sea ice. J. Glaciol., 3: 1170-1172.

Anderson, D. L. (1958) A model for determining sea ice properties. In Arctic Sea Ice, National Academy of Sciences, Washington, D.C., National Research Council, Publication 598: 198-152.

Andreas, E. L. (1980) Estimation of heat and mass fluxes over arctic leads. Mon. Wea. Rev., 108: 2057-2063.

Andreas, E. L. and S. F. Ackley (1981) On the differences in ablation seasons of the Arctic and Antarctic sea ice. J. Atmos. Sci., 39: 440-447.

Arnold, K. C. (1961) An investigation into methods of accelerating the melting of ice and snow by artificial dusting. In Geology of the Arctic, University of Toronto Press, Toronto, Ontario, Canada, Vol. 2, p. 989-1013.

Badgley, F. I. (1966) Heat balance at the surface of the Arctic Ocean. In Proceedings, Symposium on the Arctic Heat Budget and Atmospheric Circulation (J. O. Fletcher, Ed.), Rand Corp., Santa Monica, California, RM-5233-NSF, p. 215-246.

Banke, E. G., S. D. Smith and R. J. Anderson (1980) Drag coefficients at AIDJEX. In Sea Ice Processes and Models (R. S. Pritchard, Ed.), University of Washington Press, Seattle, Washington, p. 430-442.

Bilello, M. A. (1961) Formation, growth and decay of sea ice in the Canadian Arctic Archipelago. Arctic, 14: 3-24.

Brooks, C. E. P. (1949) Climate Through the Ages. McGraw-Hill, New York, 395 p.

Budyko, M. I. (1966) Polar ice and climate. In Proceedings, Symposium on the Arctic Heat Budget and Atmospheric Circulation (J. O. Fletcher, Ed.), Rand Corp., Santa Monica, California, RM-5233-NSF, p. 3-22.

Budyko, M. I. (1974) Climate and Life. International Geophysical Series 18. Academic Press, New York, 508 p.

Chernigovskii, N. T. (1966) Radiational properties of the central Arctic ice coat. Trudy Arkt. Antarkt. Nauch. Issle. Inst., 253: 249-260. (Translated by the Rand Corp., Santa Monica, California, RM-5003-PR.)
Colony, R. (1978) Daily rate of strain of the AIDJEX manned triangle. AIDJEX Bulletin, 39: 85-110.
Deardorff, J. W. (1968) Dependence of air-sea transfer coefficients on bulk stability. J. Geophys. Res., 73: 2549-2557.
Doronin, Yu. P. (1963) On the heat balance of the central Arctic. Trudy Arkt. Antarkt. Nauch. Issle. Inst., 253: 178-184.
Ewing, M. and W. L. Donn (1956) A theory of ice ages: 1. Science, 123: 1061-1066.
Ewing, M. and W. L. Donn (1958) A theory of ice ages: 2. Science, 127: 1159-1162.
Fleagle, R. G. and J. A. Businger (1963) An Introduction to Atmospheric Physics. Academic Press, New York, 346 pp.
Fletcher, J. O. (1965) The Heat Budget of the Arctic Basin and Its Relation to Climate. Rand Corp., Santa Monica, California, R-444-PR, 179 p.
Gordon, A. L. (1981) Seasonality of Southern Ocean sea ice. J. Geophys. Res., 86: 4193-4197.
Grenfell, T. C. and G. A. Maykut (1977) The optical properties of ice and snow in the Arctic Basin. J. Glaciol., 18: 445-463.
Grenfell, T. C. and D. K. Perovich (1984) Spectral albedos of sea ice and incident solar irradiance in the southern Beaufort Sea. J. Geophys. Res., 89(C3): 3573-3580.
Haltiner, G. J. and F. L. Martin (1957) Dynamical and Physical Meteorology. McGraw-Hill, New York, 470 p.
Hanson, A. M. (1965) Studies of the mass budget of arctic pack ice floes. J. Glaciol., 5: 701-709.
Houghton, H. G. (1954) On the annual heat balance of the Northern Hemisphere. J. Met., 11: 1-9.
Idso, S. B. and R. D. Jackson (1969) Thermal radiation from the atmosphere. J. Geophys. Res., 74: 5397-5403.
Kellogg, W. W. (1975) Climatic feedback mechanisms involving the polar regions. In Climate of the Arctic (G. Weller and S. A. Bowling, Ed.), Geophysical Institute, University of Alaska, p. 111-116.
Kirilova, T. V. (1952) On the dependence of the counter-radiation of the atmosphere on the degree of cloudiness. Proceedings, Main Geophysical Observatory, 37.
Laevastu, T. (1960) Factors affecting the temperature of the surface layer of the sea. Comment. Phys.-Math., 25(1): 8-134.
Langleben, M. P. (1971) Albedo of melting sea ice in the southern Beaufort Sea. J. Glaciol., 10: 101-104.
Langleben, M. P. (1972) The decay of an annual cover of sea ice. J. Glaciol., 11: 337-344.
Leavitt, E., M. Albright and F. Carsey (1978) Report on the AIDJEX meteorological experiment. AIDJEX Bulletin, 39: 121-148.

Lebedev, V. V. (1938) E
zavisimosti ot otr
Arktiki, 5: 9-25.
Leckner, B. (1978) The
the earth's surfac
143-150.
Lee, O. S. and L. S. S
ing sea ice forma
Office, Washington
Lindsay, R. W. (1976)
the arctic lead
M.S. thesis, 89 p.
Manabe, S. and R. T. W
mate change result
atmosphere. J. At
Marshunova, M. S. (1961
balance of the ur
the Arctic. Trudy
(Translated by t
RM-5003-PR, 1966.)
Martin, S. and P. Kau
ponds, or double
Mech., 64: 507-52
Maykut, G. A. (1978)
Central Arctic. J
Maykut, G. A. (1982) L
in the Central Arc
Maykut, G. A. and P. E
Alaska, 1962-66.
Maykut, G. A. and N.
the thermodynamic
changes. The R
RM-6093-PR, 173 p.
Maykut, G. A. and N. U
dependent, thermod
76: 1550-1575.
Nakawo, M. and N. K. S
of first year sea
315-330.
Ono, N. (1967) Specif
Physics of Snow a
Temperature Scie
p. 599-610.
Panov, V. V. and A.
waters on some fe
and adjacent seas.
Parkinson, C. L. and
simulated for a
Change, 2: 149-16

Lebedev, V. V. (1938) Rost l'do v arkticheskikh rekakh i moriakh v zavisimosti ot otritsatel' nykh temperatur vozdukha. Problemy Arktiki, 5: 9-25.

Leckner, B. (1978) The spectral distribution of solar radiation at the earth's surface: Elements of a model. Solar Energy, 20: 143-150.

Lee, O. S. and L. S. Simpson (1954) A practical method of predicting sea ice formation and growth. U.S. Naval Hydrographic Office, Washington, D.C., Technical Report 4, 27 p.

Lindsay, R. W. (1976) Wind and temperature profiles taken during the arctic lead experiment. University of Washington, M.S. thesis, 89 p.

Manabe, S. and R. T. Wetherald (1980) On the distribution of climate change resulting from an increase in CO_2 content of the atmosphere. J. Atmos. Sci., 37: 99-118.

Marshunova, M. S. (1961) Principal characteristics of the radiation balance of the underlying surface and of the atmosphere in the Arctic. Trudy Arkt. Antarkt. Nauch. Issle. Inst., 229. (Translated by the Rand Corp., Santa Monica, California, RM-5003-PR, 1966.)

Martin, S. and P. Kauffman (1974) The evolution of underice melt ponds, or double diffusion at the freezing point. J. Fluid Mech., 64: 507-527.

Maykut, G. A. (1978) Energy exchange over young sea ice in the Central Arctic. J. Geophys. Res., 83: 3646-3658.

Maykut, G. A. (1982) Large scale heat exchange and ice production in the Central Arctic. J. Geophys. Res., 87(C10): 7971-7984.

Maykut, G. A. and P. E. Church (1973) Radiation climate of Barrow, Alaska, 1962-66. J. Appl. Met., 12: 620-628.

Maykut, G. A. and N. Untersteiner (1969) Numerical prediction of the thermodynamic response of arctic sea ice to environmental changes. The Rand Corporation, Santa Monica, California, RM-6093-PR, 173 p.

Maykut, G. A. and N. Untersteiner (1971) Some results from a time dependent, thermodynamic model of sea ice. J. Geophys. Res., 76: 1550-1575.

Nakawo, M. and N. K. Sinha (1981) Growth rate and salinity profile of first year sea ice in the high Arctic. J. Glaciol., 27: 315-330.

Ono, N. (1967) Specific heat and heat of fusion of sea ice. In Physics of Snow and Ice, 1 (H. Oura, Ed.), Institute of Low Temperature Science, Hokkaido University, Sapporo, Japan, p. 599-610.

Panov, V. V. and A. O. Shpaikher (1964) Influence of Atlantic waters on some features of the hydrology of the Arctic Basin and adjacent seas. Deep-Sea Res., 11: 275-285.

Parkinson, C. L. and W. M. Kellogg (1979) Arctic sea ice decay simulated for a CO_2-induced temperature rise. Climatic Change, 2: 149-162.

Parkinson, C. L. and W. M. Washington (1979) A large scale model of sea ice. J. Geophys. Res., 84: 311-337.

Perovich, D. K. and T. C. Grenfell (1981) Laboratory studies of the optical properties of young sea ice. J. Glaciol., 27: 331-346.

Richards, J. M. (1971) A simple expression for the saturation vapour pressure of water in the range -50° to 140°C. Brit. J. Appl. Phys., 4: L15-L18.

Rigby, F. A. and A. Hanson (1976) Evolution of a large arctic pressure ridge. AIDJEX Bulletin, 34: 43-71.

Schwarzacher, W. (1959) Pack ice studies in the Arctic Ocean. J. Geophys. Res., 64: 2357-2367.

Schwerdtfeger, P. (1963) The thermal properties of sea ice. J. Glaciol., 4: 789-807.

Semtner, A. J. (1976) A model for the thermodynamic growth of sea ice in numerical investigations of climate. J. Phys. Oceanogr., 6: 379-389.

Shine, K. P. (1984) Parameterization of shortwave flux over high albedo surfaces as a function of cloud thickness and surface albedo. Q. J. R. Meteorol. Soc., 110: 747-760.

Thorndike, A. S., D. A. Rothrock, G. A. Maykut and R. Colony (1975) The thickness distribution of sea ice. J. Geophys. Res., 80: 4501-4513.

Thorndike, A. S. and J. Y. Cheung (1977) AIDJEX measurements of sea ice motion. AIDJEX Bulletin, 35: 1-149.

Thorndike, A. S. and R. Colony (1980) Arctic Ocean buoy program, 19 January 1979 - 31 December 1979. Polar Science Center, University of Washington, 131 p.

Thorndike, A. S. and R. Colony (1981) Arctic Ocean buoy program, 1 January 1980 - 31 December 1980. Polar Science Center, University of Washington, 132 p.

Thorndike, A. S., R. Colony and E. A. Munoz (1983) Arctic Ocean buoy program, 1 January 1981 - 31 December 1981. Polar Science Center, University of Washington, 137 p.

Thorndike, A. S., R. Colony and E. A. Munoz (1983) Arctic Ocean buoy program, 1 January 1982 - 31 December 1982. Polar Science Center, University of Washington, 132 p.

Thorpe, M. R., E. G. Banke and S. D. Smith (1973) Eddy correlation measurements of evaporation and sensible heat flux over arctic sea ice. J. Geophys. Res., 78: 3573-3584.

Untersteiner, N. (1961) On the mass and heat budget of arctic sea ice. Arch. Met. Geophys. Bioklim., A(12): 151-182.

Untersteiner, N. (1962) The ice budget of the Arctic Ocean. Proceedings of the Arctic Basin Symposium, Arctic Institute of North America, p. 219-226.

Untersteiner, N. (1964) Calculations of temperature regime and heat budget of sea ice in the Central Arctic. J. Geophys. Res., 69: 4755-4766.

Untersteiner, N. and F. Badgley (1965) The roughness parameters of sea ice. J. Geophys. Res., 70: 4573-4577.

Vowinckel, E. and S. Or
ation income and c
552-559.

Vowinckel, E. and S. (
radiation at the
Montreal, Publicat

Vowinckel, E. and S. O
Arctic. McGill U
ology No. 51, 27 p

Vowinckel, E. and S. O
Beaufort Sea. In
Meteorological Org

Wadhams, P. and R. J.
obtained by submar
Sea. Scott Polar
65 p.

Walker, E. R. and P. W
32: 140-147.

Weller, G. (1972) Radi
14: 28-30. (Av
Information Servic

Wiscombe, W. J. (1975
summer stratus c
Weller and S.
University of Alas

Wittmann, W. I. and J.
of arctic pack ic
Heat Budget and
Ed.), Rand Corp.
215-246.

Yen, Y. C. (1981) Rev
sea ice. USA-CRR

Zillman, J. W. (1972)
heat budgets of t
logical Studies,
Interior, Canberr

Zubov, N. N. (1945) I
Glavsevmorputi),
Office, Translat
NTIS, Springfield

979) A large scale model
11-337.
l) Laboratory studies of
ice. J. Glaciol., 27:

sion for the saturation
-50° to 140°C. Brit. J.

ıtion of a large arctic
43-71.
s in the Arctic Ocean.

erties of sea ice. J.

rmodynamic growth of sea
climate. J. Phys.

shortwave flux over high
d thickness and surface
747-760.
cut and R. Colony (1975)
. J. Geophys. Res., 80:

)JEX measurements of sea
49.
tic Ocean buoy program,
Polar Science Center,

ic Ocean buoy program,
Polar Science Center,

oz (1983) Arctic Ocean
December 1981. Polar
n, 137 p.
oz (1983) Arctic Ocean
December 1982. Polar
n, 132 p.
(1973) Eddy correlation
e heat flux over arctic
34.
budget of arctic sea
): 151-182.
of the Arctic Ocean.
m, Arctic Institute of

rature regime and heat
. J. Geophys. Res.,

oughness parameters of
77.

Vowinckel, E. and S. Orvig (1962a) The relation between solar radiation income and cloud type in the Arctic. J. Appl. Met., 1: 552-559.

Vowinckel, E. and S. Orvig (1962b) Insolation and absorbed solar radiation at the ground in the Arctic. McGill University, Montreal, Publication in Meteorology No. 53, 50 p.

Vowinckel, E. and S. Orvig (1962c) Cloud amount and type over the Arctic. McGill University, Montreal, Publication in Meteorology No. 51, 27 pp.

Vowinckel, E. and S. Orvig (1972) Synoptic energy budgets from the Beaufort Sea. In Energy Fluxes over Polar Surfaces. World Meteorological Organization, Geneva, p. 143-166.

Wadhams, P. and R. J. Horne (1978) An analysis of ice profiles obtained by submarine sonar in the AIDJEX area of the Beaufort Sea. Scott Polar Research Institute, Technical Report 78-1, 65 p.

Weller, E. R. and P. Wadhams (1979) Thick sea ice floes. Arctic, 32: 140-147.

Weller, G. (1972) Radiation flux investigation. AIDJEX Bulletin, 14: 28-30. (Available as PB 220/859, National Technical Information Service, Springfield, Virginia.)

Wiscombe, W. J. (1975) Solar radiation calculations for arctic summer stratus conditions. In Climate of the Arctic (G. Weller and S. A. Bowling, Ed.), Geophysical Institute, University of Alaska, p. 245-254.

Wittmann, W. I. and J. J. Schule (1966) Comments on the mass budget of arctic pack ice. In Proceedings, Symposium on the Arctic Heat Budget and Atmospheric Circulation (J. O. Fletcher, Ed.), Rand Corp., Santa Monica, California, RM-5233-NSF, p. 215-246.

Yen, Y. C. (1981) Review of thermal properties of snow, ice and sea ice. USA-CRREL Res. Rept. 81-10, Hanover, NH, 27 p.

Zillman, J. W. (1972) A study of some aspects of the radiation and heat budgets of the Southern Hemisphere oceans. In Meteorological Studies, 26, Bureau of Meteorology, Department of the Interior, Canberra, Australia, 562 p.

Zubov, N. N. (1945) L'dy Arktiki. (Arctic Ice.) (Izdatel'stvo Glavsevmorputi), Moscow, 360 p. (U.S. Navy Hydrographic Office, Translation 217, 1963; available as AD426972 from NTIS, Springfield, VA.)